scientific reports

Check for updates

OPEN

# SEOR2 in *Arabidopsis* mediates $Ca^{2+}$ dependent defense against phytoplasmas and reduction of plant growth

Keziah Omenge[1,6], Ottone Carmelo Viscardo[2,3,6], Fernando Rodrigo De Oliveira Cantao[4], Simonetta Santi[4], Aart Jan Eeuwe van Bel[5] & Rita Musetti[2]✉

**The *Arabidopsis seor1ko* line, which expresses the protein AtSEOR2 free of its bond with AtSEOR1, exhibits a lower phytoplasma titre as compared to wild type plants. In search for mechanism(s) underlying potential SEOR2-mediated defense responses the transcriptome of healthy wild type and *Atseor1ko* plants was disclosed by RNA sequencing. Comparative transcriptome analysis revealed 1036 differentially expressed genes (DEGs, 893 up- and 143 down-regulated) between the *Atseor1ko* line and the wild type. Sequence annotation and classification of the up-regulated genes identified "plant-pathogen interaction" among the most enriched clusters. The "plant-pathogen interaction" cluster included genes encoding members of the protein kinase superfamily, actors in calcium/calmodulin signaling transduction and WRKY transcription factors. An interaction network analysis and a host-phytoplasma interaction map demonstrated that AtSEOR2 protein could interact with the calcium-binding proteins CAM2 and TCH3. The latter one also turned out to be an indirect target of the $SAP54_{CY}$ phytoplasma effector, which suggests a SEOR2-mediated role of TCH3 in balancing nutrient investments in plant defense and plant growth.**

**Keywords** *Arabidopsis*, AtSEOR2, Effectors, Interaction, Phloem, Plant defense, Phytoplasma

Phytoplasmas are sieve-element (SE) restricted pathogenic prokaryotes[1] causing severe yield and/or quality loss of many economically important crops[2]. Thus far, phytoplasma epidemics are mainly combatted by insect vector control through pesticides, or by removal of symptomatic plants. However, the efficacy of these approaches is limited because chemical control of vector proliferation is often inadequate and natural phytoplasma reservoirs in host plants are unknown or reside in nearby wild plants[3]. Thus, there is an urgent need for novel ways to control phytoplasma infections. Such strategies, however, require a profound knowledge of the complex mechanisms that underlie plant-phytoplasma relationships. Studies on the molecular interaction between phytoplasmas and host plants would provide important information for development of more efficient and sustainable control strategies based on natural plant defense mechanisms[4].

Phytoplasmas heavily affect host physiology by secretion of chemical effectors that weaken the defense responses of the host[5]. Effectors are able to move systemically via the SEs or to migrate cell-to-cell from the SEs to adjacent cells and tissues[6]. Plants dispose of receptor proteins for early recognition of effectors mediating plant immune reactions that counteract host colonization[7]. For phytoplasma-plant host interaction, it is unknown whether and how effector-recognition proteins activate an effector-triggered immunity (ETI). Natural resistance mechanisms to phytoplasma diseases have not yet been detected among cultivated plants, but their existence is likely, given the diverse levels of susceptibility between the genotypes of one species[8–10].

A limited number of studies, mainly making use of model plants, provided a few interesting candidate genes to be exploited in the search for resistance mechanisms against phytoplasma infection[11,12]. Phytoplasma quantification in different lines of *Arabidopsis thaliana* showed that the *Atseor1ko* line, expressing the protein

[1]Institute for Biosafety in Plant Biotechnology (SB), Julius Kühn-Institut (JKI) - Federal Research Centre for Cultivated Plants, Erwin-Baur-Straße 27, 06484 Quedlinburg, Germany. [2]Department of Land, Environment, Agriculture and Forestry (TESAF), University of Padova, Viale Dell'Università 16, 35020 Legnaro, PD, Italy. [3]CREA Centro di Ricerca per la Viticoltura e l'Enologia, Via XXVIII Aprile 26, 31015 Conegliano, TV, Italy. [4]Department of Agricultural, Food, Environmental and Animal Sciences, University of Udine, Via delle Scienze 206, 33100 Udine, Italy. [5]Institute of Phytopathology, Justus-Liebig University, Heinrich-Buff-Ring 26–32, 35392 Giessen, Germany. [6]Keziah Omenge and Ottone Carmelo Viscardo have contributed equally to this work. ✉email: rita.musetti@unipd.it

AtSEOR2 (gene locus At3g01670), that is non-conjugated in the absence of its natural partner AtSEOR1 (gene locus At3g01680)[13], exhibits a lower titre of *Chrysanthemum yellows* (CY) phytoplasma as compared to wild-type plants[11]. Suppression of phytoplasma proliferation suggests that SEOR2 strengthens in some way plant immune processes from the early stage of infection on[11,12]. Moreover, the capability of AtSEOR2 to interact with several proteins involved in pathogen perception and in associated defense responses has recently been underscored[14]. Hence, AtSEOR2 was defined as "one of the effector hubs involved in plant immunity" in *Arabidopsis*[14]. As a matter of fact, AtSEOR2, detached from AtSEOR1, interacts with plant resistance proteins in yeast-two hybrid assays[15–17]. This all suggests that AtSEOR2 acts in the defense cascade during phytoplasma infection[18].

The intriguing potential of AtSEOR2 called for further investigations on the molecular traits of the *Atseor1ko* line to unveil details of the involvement of AtSEOR2 in defense responses to CY phytoplasmas. Therefore, the transcriptome of wild type and *Atseor1ko* plants was obtained by RNA sequencing (RNA-seq) of healthy leaf tissues. The expression patterns of 17 genes, that were differentially expressed in wild-type and mutant plants and are engaged in calcium and hormone signal transduction pathways early in response to pathogen infection[12], were evaluated by reverse transcriptase-quantitative PCR (RT-qPCR). The expression level of the $SAP54_{CY}$ phytoplasma effector was also determined in infected wild-type and mutant plants. Using the Host–Pathogen Interaction Data Base 3.0 (HPIDB 3.0) program, a protein–protein interaction network and a host-phytoplasma interaction map were constructed to reveal possible SEOR2 interactors having a role in the defense response of the plant.

## Results

### Transcriptome profiles of healthy wild-type and *Atseor1ko* plants

Using 5 biological replicates for either plant line (wild type or *Atseor1ko*) a total of 10 RNA-seq libraries of *Arabidopsis* wild type and *Atseor1ko* leaf rosettes were constructed. The quality scores 30 (Q30 values) were all above 95% in all 10 libraries indicating that the RNA-seq experiment produced high-quality and reliable data. Based on the gene expression data obtained from fragments per kilobase of exon per million reads mapped, a principal component analysis (PCA) was performed and a heatmap was constructed. The analysis showed that the wild type and *Atseor1ko* samples were clustered into 2 groups. This indicated that wild type plants and *Atseor1ko* mutants exhibit clearly distinct transcriptional expression patterns. Following the PCA analysis outliers were identified, so that 3 libraries for the wild type and 4 for the *Atseor1ko* lines were taken for a follow-up transcriptome analysis (Fig. 1A,B). To obtain accurate profiles of the differentially expressed genes (DEGs), the cutoff was set at an adjusted $p$-value < 0.05 ($p_{adj} < 0.05$) and an absolute fold change (FC) ≥ 2. DEGs were visualized as an MA-plot, constructed by a plot of log-fold change (M-values, *i. e.* the log of the ratio of level counts for each gene between control and mutant samples) against the log-average (A-values, *i. e.* the average level counts for each gene across the control and mutant samples (Fig. 1C). DESeq2-based analysis showed that 1036 genes in the *Atseor1ko* mutants were differentially expressed as compared to the wild type plants. The majority of DEGs, 893 (86.2% of the total), were up-regulated in *Atseor1ko* mutants, while 143 genes were down-regulated (13.8% of the total) (Fig. 1D). The up-regulated genes were screened in more detail to assess potential involvement in *Arabidopsis* defense mechanisms.

### Knocking out the *AtSEOR1* gene induces considerable changes in the transcriptome of *Arabidopsis* leaves

To gain further insight into the transcription profile of *Atseor1ko* plants, we classified the DEGs according to the Gene Ontology (GO) terms (Fig. 2) and the Kyoto Encyclopedia of Genes and Genomes [KEGG,[19]] categories (Fig. 3A). Regarding the GO terms, the majority of "Biological process" terms represented "cellular processes" (Fig. 2A), the majority of "Cellular components" terms represented "cellular anatomical entity" (Fig. 2B) and the majority of "Molecular function" terms represented "binding" and "catalytic activity" (Fig. 2C). On the basis of DEGs, KEGG analysis identified the most enriched pathways in *Atseor1ko* mutants in comparison to wild-type plants. These enriched pathways were: "biosynthesis of secondary metabolites", "plant pathogen interaction", "plant hormone signal transduction", "starch and sucrose metabolism", "MPK signaling pathway-plant", "phenylpropanoid biosynthesis", "photosynthesis—antenna proteins", "carotenoid biosynthesis", "alpha-linoleic acid metabolism", "zeatin biosynthesis", "linoleic acid metabolism" (Fig. 3A). Among these categories, those belonging to "plant-pathogen interaction" and "MPK signaling" were among the most significantly enriched in the *Atseor1ko* plants (Fig. 3A). In fact, several genes encoding proteins participating in calcium perception and signal transduction were significantly over-expressed in the *Atseor1ko* line, such as genes encoding calmodulins/calmodulin-like proteins, protein kinases and WRKY transcription factors (Fig. 3B; Table 1). The up-regulated calcium/calmodulin signaling group encompasses genes encoding calcium-binding EF-hand family proteins, such as the calmodulin-like (CML) proteins TCH2 (also called CML24), TCH3 (CML12), CML16, CML23, CML37, CML38, CML40, CML49, MSS3 (CML5) (Table 1); the calcium-dependent protein kinases, CPK28, CPK29, CPK32, the calmodulin 2 (CAM2), the cyclic nucleotide gated channels 14 and 19 (CNGC14 and CNGC19) (Table 1). The up-regulated protein kinase superfamily group includes genes encoding the mitogen-activated protein kinase 3 (MPK3), the *Pseudomonas syringae pv tomato* (Pto)-interacting protein kinase 1–4 (PTI1-4, also called CARK3), PTI1-2 (CARK5), CARK6 and the AGC protein kinase AGC2-1. The up-regulated WRKY transcription factor cluster is composed of WRKY DNA-binding protein 33 (WRKY33) and WRKY family transcription factor 22 (WRKY22) (Table 1).

Among the enriched clusters, the "hormone signal transduction" group includes genes related to plant responses to phytoplasma, even during the early stage of infection[12]. This group comprises numerous phytohormone-responsive genes, such as the auxin-responsive genes *SAUR, AUXIN/INDOLE ACETIC ACID (Aux/IAA)* and *GRETCHEN HAGEN3 (GH3)* families. For instance, *SAUR48*, *IAA6*, *IAA19*, *GH3.1* were among the most up-regulated genes in *Atseor1ko* plants in comparison with the wild-type (Table 2).

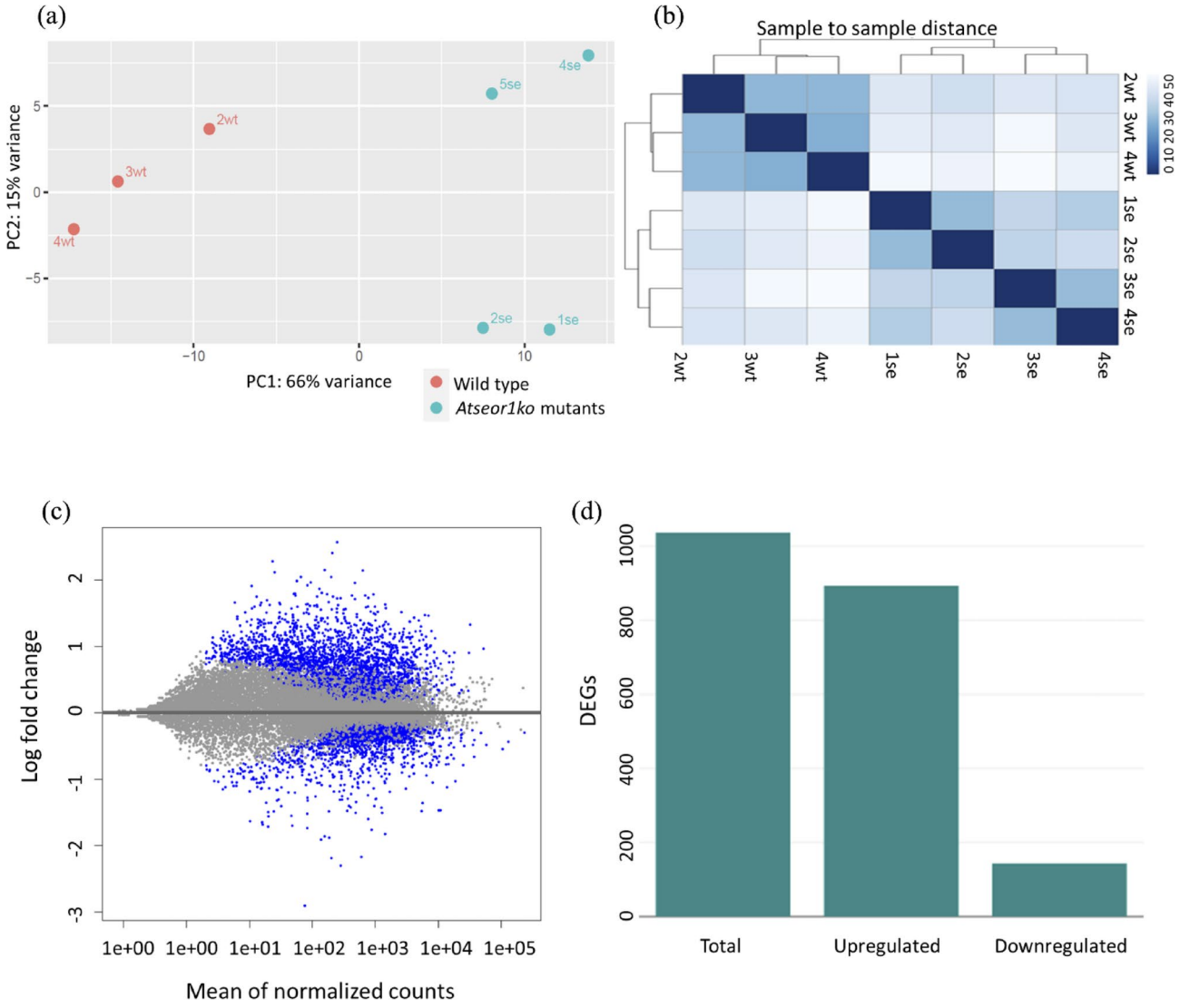


**Fig. 1**. Aggregate RNA transcripts of wild type plants and of *Atseor1ko* mutants and gene expression profiles of *Atseor1ko* mutants. (**A**) Principal component analysis (PCA) scatter plot of gene expression shows the variance among the biological replicates in each genotype. Percentages on each axis represent the percentages of variation explained by the principal components. (**B**) Expression heatmap of sample-to-sample distance matrix as calculated from the variance stabilizing transformation of count data for transcripts of wild type and *Atseor1ko* groups. (**C**) MA plot of log-fold change (M-values, i. e. the log of the ratio of level counts for each gene between the two samples) against the log-average (A-values, *i. e.* the average level counts for each gene across the two samples). The differentially expressed genes (DEGs) in *Atseor1ko* vs. wild-type plants are indicated in blue. Genes with similar expression levels in the two sample groups (in grey) are assembled scattered along the X-axis. (**D**) Amounts of differentially expressed genes (DEGs) in *Atseor1ko* plants, grouped as total DEGs, up-regulated DEGs and down-regulated DEGs. Significantly DEGs are those limited by the adjusted *p*-value ($p_{adj}$) < 0.05 and the absolute fold change ≥ 2.

As for the regulation of cytokinin, jasmonates (JA) and salicylic acid (SA) activity, the *Arabidopsis Response Regulator* 5 *(ARR5)* gene, encoding a cytokinin regulator of A*RR* gene family, was also a significant overexpressed gene in the mutant line, as well as the *JAZ1* and *JAZ5* genes, which respectively encode the JASMONATE-ZIM DOMAIN (JAZ) repressor proteins 1 and 5 (Table 2). *COI1*, encoding a JAZ-degrading protein, was not modulated. Moreover, *ACS6*, which encodes an enzyme of the ethylene (ET) biosynthetic pathway, was significantly up-regulated in *Atseor1ko* plants (Table 2). Of the SA-related genes, only *NPR3* was found to be modulated in the mutant line in comparison with the wild type, which resulted in a significant up-regulation (Table 2).

## Validation of DEGs

RT-qPCR was performed to validate the transcriptional profiles of 17 genes obtained by RNA-seq (Supplementary Table 1). In addition to some of the genes participating in calcium perception and signaling (such as *CAM2*,

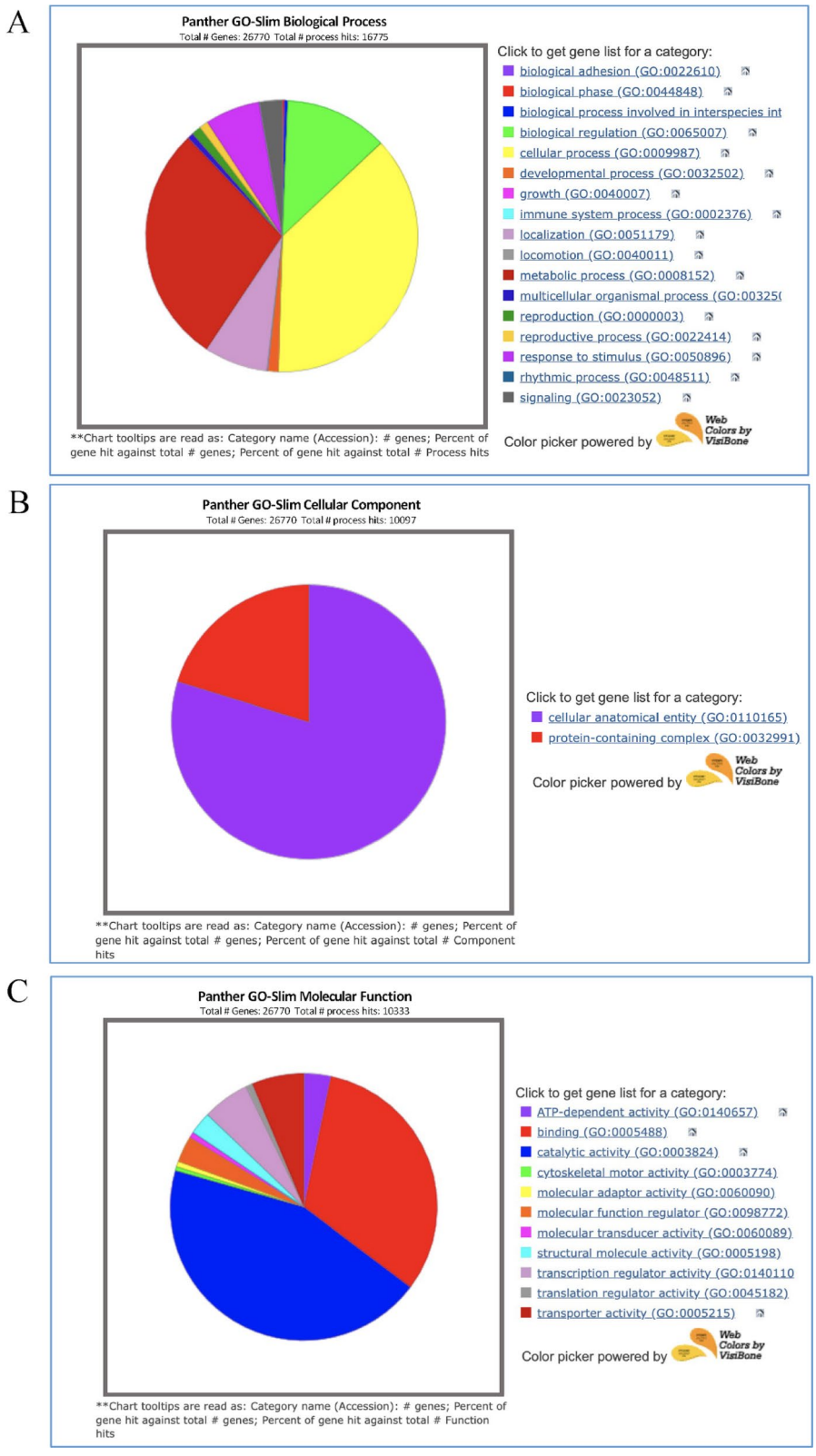


**Fig. 2**. Gene Ontology (GO) term enrichment analysis of differentially expressed genes (DEGs). Significantly enriched GO terms were selected based on $p$-value < 0.05. GO term annotations encompassing the three principal GO categories: (**A**) "Biological process", (**B**) "Cellular component", (**C**) "Molecular function". The majority of "Biological process" terms represents "cellular process", the majority of "Cellular component" terms represents "cellular anatomical entity" and the majority of "Molecular function" terms represent "binding" and "catalytic activity".

*CML37*, *CML40*, *CML49*, *TCH2*, *TCH3*, *MPK3*, *AGC2-1*, *WRKY22*), (Table 1), we included others related to effector-triggered immunity (ETI) (*RPS4*, *RBOH-D* and *RBOH*-F) and phytohormone signal transduction (*COI1, NPR3, JAZ1, SAUR48* and *ACS6*) pathways (Table 2).

The analysis perfectly matched the patterns generated by RNA-seq (Fig. 3C). Genes encoding proteins related to calcium perception and signaling, and encoding the WRKY22 transcription factor were expressed to a significantly higher degree in the *Atseor1ko* line in comparison with the wild type (*CAM2* + 65%, *CML37* + 207%, *CML40* + 212%, *CML49* + 61%, *TCH2* + 180% and *TCH3* + 116%, *MPK3* + 51%, *AGC2-1* + 73%, *WRKY22* + 75%) (Fig. 4). Among the genes related to phytohormone signaling, *NPR3, JAZ1, SAUR48* and *ACS6* were confirmed to be significantly overexpressed in the mutant line (+ 136%, + 119%, + 717% and + 229% respectively), whereas expression of *COI1* remained similar (Fig. 5A).

Expression of other defense-related plant genes such as *RBOH-D* and *RBOH-F* was not modulated in the mutant line in comparison with the wild type (Fig. 5B) just as the resistance to *Pseudomonas syringae protein 4* gene, *RPS4*, which encodes an LRR receptor.

## Construction of AtSEOR2 interaction network and host-phytoplasma interaction map

RNA-seq experiments enabled us to identify 1036 DEGs in *Atseor1ko* mutants. These genes encode a range of proteins, the interaction of which with AtSEOR2 protein and phytoplasma effectors is unknown. To identify potential interactions, host–pathogen interaction network analyses were carried out by use of HPIDB 3.0[20]. This model assumes that protein X and Y are an interacting pair if their homologs X' and Y' are known to be an interacting pair. Previous studies showed that proteins with 30% sequence similarity can interact with each other[21]. Therefore, we predicted the interaction of proteins with 30% sequence identity and 1e-5 E-value through HPIDB 3.0 and Blosum45 matrix[20]. After filtering out spurious interactions from the whole dataset, a total of 445 proteins remained. After removal of 331 redundant proteins, 114 unique interacting proteins remained. Among these, we distinguished 33 phytoplasma proteins (SAPs or effectors) and 30 AtSEOR2-related proteins. The analysis evidenced that AtSEOR2 can interact with *Arabidopsis* proteins involved in calcium/calmodulin signal transduction. In particular, AtSEOR2 would strongly interact with CAM2, TCH3 and indirectly with CML49 (Fig. 6A).

Moreover, network analysis highlighted a possible indirect interaction of the calcium-binding EF-hand family protein TCH3 with the phytoplasma $SAP54_{CY}$ effector (Fig. 6B), which appears to be mediated by the SOC1 protein.

## Transcripts of *SAP54*$_{CY}$ are abundant in CY-infected wild-type and *Atseor1ko* lines.

The secretion of effector proteins by phytoplasmas is fundamental for the establishment of the interactions with plant hosts and insect vectors. To evaluate the potential influence of differences between hosts (wild-type vs mutant line) on the expression profile of the phytoplasma effector gene $SAP54_{CY}$, we tested the abundance of $SAP54_{CY}$ transcripts in wild type and *Atseor1ko Arabidopsis* lines subjected to feeding by infectious insect vector. The analyses demonstrated the presence of CY phytoplasmas and $SAP54_{CY}$ transcripts in these *Arabidopsis* lines treated with infectious vectors (Supplementary Tables 3 and 4). The expression levels of $SAP54_{CY}$ were not significantly different in the two infected *Arabidopsis* lines (Fig. 7) and the $SAP54_{CY}$ transcripts were not detected in the corresponding healthy control plants (Supplementary Table 4).

## Discussion

It is beyond doubt that sieve element occlusion (SEO) proteins, orderly framed in so-called forisomes, are responsible for the sieve-plate occlusion in legumes[22,23]. By contrast, it is a matter of debate, if SEOR1 and SEOR2 in loosely arranged skein shape, as in the sieve tubes of *Arabidopsis* and in other dicots[24], are capable of a similar occlusion achievement. It seems that these fibrillar proteins do not obstruct phloem flow in unchallenged sieve tubes[25] in line with the inactivity of contracted forisomes[22]. As in damaged or disturbed legume sieve tubes, however, filamentous AtSEOR1 and AtSEOR2 may undergo $Ca^{2+}$-mediated conformation changes that lead to sieve-pore occlusion by protein plugs[11,26,27]. The clogging probably requires a specific $Ca^{2+}$-mediated conjugation of both AtSEOR fibrillar species and is regarded as a fast and efficient strategy to impair phloem translocation[11,28].

Detached from AtSEOR1, AtSEOR2 may perform a function other than sieve-pore occlusion in view of the decreased pathogen titers in phytoplasma-infected *Atseor1ko* plants[11,12]. Hence, it was speculated that, in absence of AtSEOR1, AtSEOR2 in its unbound form is involved in plant immune signaling, through an interaction with other defense-related plant compounds ([18] and references therein) and/or with phytoplasma effectors[14].

Since the effectiveness of the plant response is related to constitutive or pro-active defense mechanisms[29], a comparative RNA-seq analysis was conducted between uninfected wild-type and *Atseor1ko Arabidopsis* plants.

Bioinformatic analysis, followed by PCA, revealed different transcriptional patterns between *Atseor1ko* mutants and wild-type plants. Sequence annotation and DEG classification, obtained from GO categories and KEGG pathway analysis, evidenced that the most enriched pathways in *Atseor1ko* line are those related to signaling mechanisms and defense responses. In particular, transcripts encoding proteins involved in calcium binding, calcium/calmodulin signaling and hormone signal transduction are among the most enhanced in the mutants.

In the following sections, a broader perspective on the transcript clusters that are among the most up-regulated ones ("calcium-signaling pathway" and "phytohormone signal transduction") in *Atseor1ko* mutants, is sketched by using the wealth of existing reports on the functions of the genes in question.

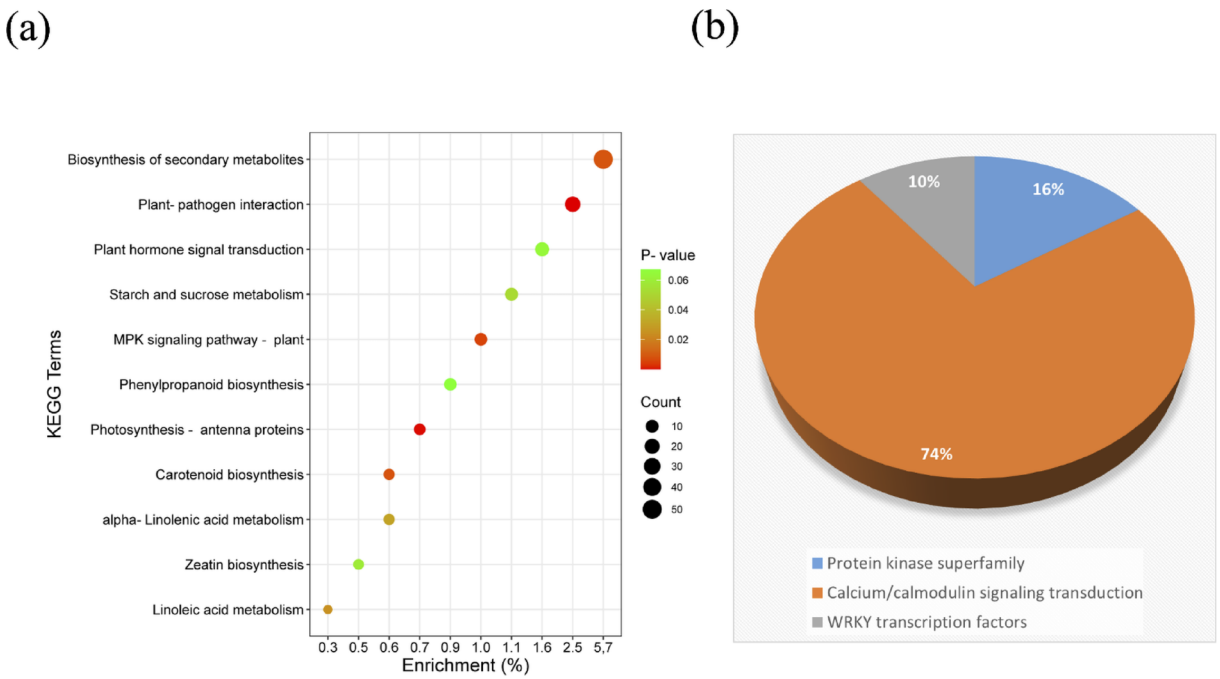


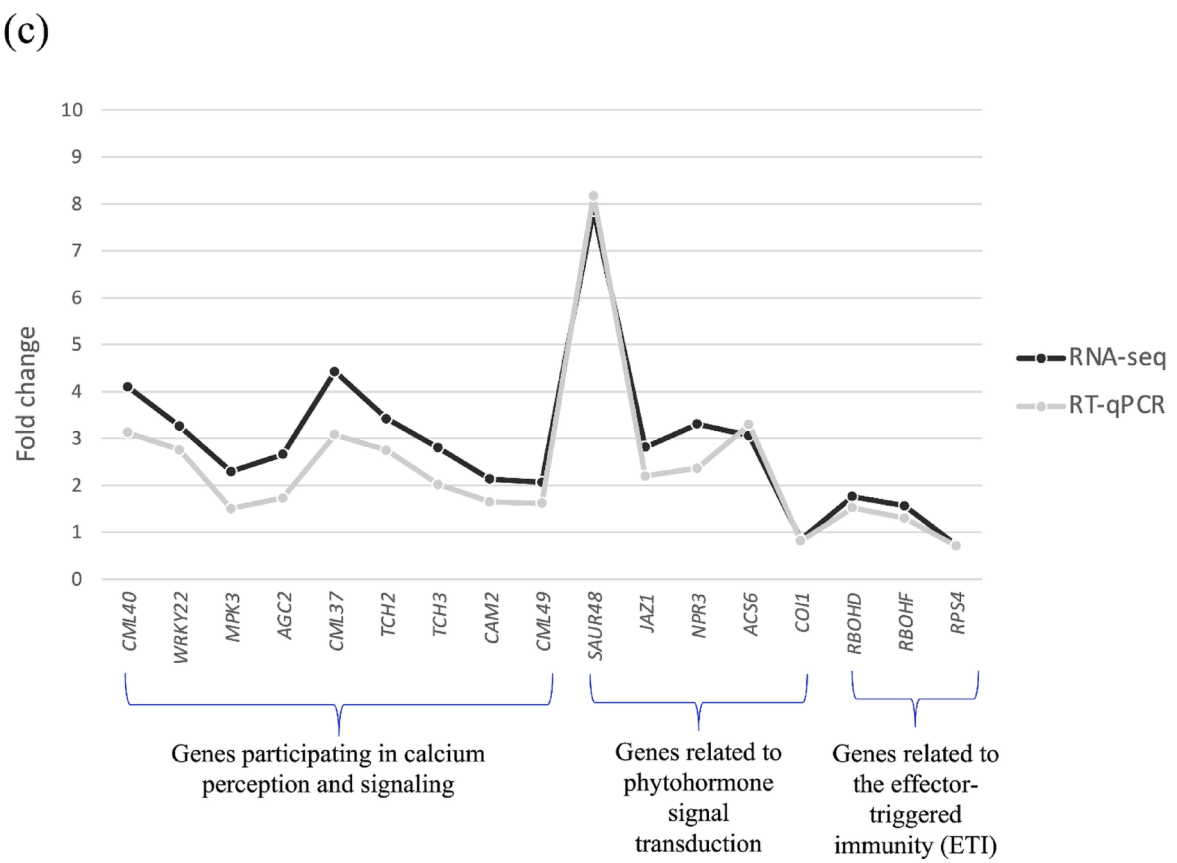


## The calcium-mediated signaling pathway is activated in the *Atseor1ko* line

*Putative functions of the up-regulated genes encoding calmodulin-like proteins, $Ca^{2+}$-dependent protein kinases and protein kinases*

Changes in $Ca^{2+}$ level in the cytosol, provoked by various environmental stimuli, are recognized and processed by $Ca^{2+}$-sensor proteins, which have been identified as crucial hubs in signal transduction[30]. Following RNA-seq analysis, numerous genes, encoding $Ca^{2+}$-sensor proteins like calmodulins (CAMs), calmodulin-like (CML) proteins, $Ca^{2+}$-dependent protein kinases (CPKs) and protein kinases were up-regulated in *Atseor1ko* mutants. *CAM2*, *CML37*, *CML38*, *CML16*, *CML23*, *CML40*, and *CML49* were the most up-regulated genes, which are

◀**Fig. 3**. Kyoto Encyclopedia of Genes and Genomes (KEGG) enrichment analysis of the RNA-seq data and validation of RNA-seq by RT-qPCR of differentially expressed genes. (**A**) The 11 pathways from the KEGG enrichment analysis ranked by *p*-value, shown as a dot chart. The terms of the KEGG pathways are depicted on the y-axis. The shared number of pathways is shown as the dot sizes. The colors distinguish the *p*-value classes. A pathway for the DEGs was defined as significantly enriched pathway when its $p$-value < 0.05. The smaller the *p*-value, the more significant is the pathway change. (**B**) Pie chart representing the proportion of the members of the "plant-pathogen interaction" cluster. (**C**) The mean fold-change value (on log2 basis) for each group was compared for 17 genes that belong to the three categories at the bottom of the figure. RT-qPCR data was normalized by UBC9 expression for each sample. Means of significant ($p < 0.05$) fold changes were computed for RT-qPCR and DESeq using at least three technical replicas for each plant in each analysis.

related to $Ca^{2+}$ signaling in *Arabidopsis* in response to biotrophic pathogen attack or aphid infestation[31,32]. Other up-regulated calmodulin-like genes such as *TCH2* are also activated in response to mechanical stresses or, as *TCH3*, are involved in the regulation of the auxin efflux and polar transport[33]. TCH2 and TCH3 also cooperate with several calcium-sensors for decoding immune-related calcium signals and participate in plant immune response[34,35]. The calmodulin CAM2 is able to interact with numerous structurally distinct targets[36], among which the $Ca^{2+}$ channel CNGC19 (*CNGC19* also resulted up-regulated in our work), leading to increasing cytosolic $Ca^{2+}$ levels[37]. Calmodulin-CNGC complexes and the associated calcium-signaling cascades are activated by diverse CPKs[38] with diverse regulatory functions in the $Ca^{2+}$-mediated hormonal signaling pathway[38] and, hence, are not only engaged in the defense mechanisms, but also in the developmental plant processes[39]. As for the protein kinase superfamily, this group of proteins works downstream of sensors/receptors and transforms stimuli—along with a signal amplification—into responses. In *Arabidopsis*, the constitutive activation of protein kinase genes (like *MPK3*) triggers early defense responses to bacterial and fungal pathogens[40] by phosphorylation of transcription factors, such as WRKY33 and WRKY22[41], and hormonal biosynthetic enzymes, for instance ACS2 and ACS6, involved in ethylene biosynthesis[42,43]. All in all, up-regulation of the expression of this gene category by AtSEOR2 seems to enhance the defense efforts of the host.

## Hormone-mediated signal transduction pathways are repressed in the *Atseor1ko* line

*Putative functions of the up-regulated genes encoding hormonal receptors and hormone-sensitive enzymes*

RNA-seq also evidenced that several genes encoding hormonal receptors were significantly over-expressed in *Atseor1ko* plants (Table 2). *SAUR*, *AUX/IAA*, and *GH3* form a co-receptor complex involved in the early transcriptional repression of auxin[44,45], whereas *ARR5* encodes a negative regulator of the cytokinin signaling[46]. Auxin and cytokinin play fundamental roles in plant growth and development[47] and their synthesis induces a rapid, but transient increase of the cytosolic $Ca^{2+}$ concentration in various plant species. So, receptor proteins are surmised to act as functional and integrative hubs between the $Ca^{2+}$ level and auxin-/cytokinin-related responses[48,49]. All in all, it seems that the auxin and cytokinin signaling is suppressed in *Atseor1ko* rosettes, via the modulation by a pool of repressor genes. JA and SA also play crucial roles in plant growth and organ differentiation, especially flowering[50]. Both JA and SA signaling pathways are affected in the *Atseor1ko* line in comparison with the wild type. The expression of the JA repressor genes (*COI1*, *JAZ1* and *JAZ5*) indicates the shutdown of JA synthesis in the mutant line and this is consistent with the similar JA-Ile and JA contents between the wild type and *Atseor1ko* lines previously reported[12]. *NPR3* encodes a protein which promotes the NPR1 homeostasis[51], balancing the regulation of the SA-dependent defense responses and growth processes[52]. In conclusion, AtSEOR2-induced up-regulation of this gene set seems to limit the growth efforts of the host.

## An over-all assessment of the consequences of AtSEOR1 absence

Collectively, the results indicate that $Ca^{2+}$ sensors, $Ca^{2+}$ processors and other downstream regulators are up-regulated in *Atseor1ko* plants to promote the production of antimicrobial compounds. Moreover, the ABA-mediated signaling pathway, which, in turn, regulates ethylene biosynthesis[53] seems to be stimulated, whereas IAA-, cytokinine-, jasmonate- and salicylate-mediated signaling pathways are suppressed in *Atseor1ko* plants. All in all, it appears that AtSEOR2 interacts with a crucial hub (called here "transcriptional regulatory platform", Fig. 8) that controls the balance between plant growth and stress tolerance by steering the division of energy investment between growth and defense achievements[51,54].

There is some support for a role of *SEOR2* in plant growth efforts. The Atinian VA-AP38 genotype of *Ulmus minor* is highly susceptible to the Dutch elm disease since it develops exceptionally wide earlywood vessels[55]. In this clone, transcripts of an *SEOR2* gene homolog figured among the top 25 down-regulated genes during *Ophiostoma novo-ulmi* infection[55], with significantly low expression values when wilt symptoms had advanced into the tree crown. A specific function was not attributed to the *SEOR* gene homolog, but according to microarray analysis, it belongs to a gene cluster related to growth, in particular to the synthesis and architecture of the secondary cell wall[55], which is supportive for a role of SEOR2 in plant growth.

The mode of interaction between AtSEOR2 and the putative "transcriptional regulatory platform" is fully unknown. SEOR proteins possess a conserved "potential thioredoxin fold" characterized by the absence of two central cysteine residues, a characteristic feature of $Ca^{2+}$ binding proteins[56]. The function of $Ca^{2+}$ binding proteins, in general, is the regulation of the activity of other proteins by a $Ca^{2+}$-dependent interaction[57]. Calcium binding induces conformational transitions in proteins, that make them specifically active to particular targets[58]. Moreover, SEOR proteins have an "intrinsec disorder domain"[24] which is characteristic of regulatory proteins, and often constitute "hubs" which can potentially regulate entire signaling pathways[59]. A network analysis by the HPIDB program predicted interaction of AtSEOR2 with CAM2, TCH3 (direct) and CML49 (indirect). These

| Gene ID | baseMean | log2FoldChange | $p_{adj}$ | Gene symbol | KEGG\|NCBI Refseq description |
|---|---|---|---|---|---|
| AT1G01340 | 260.930 | − 0.912 | 0.0000 | CNGC10 | K05391 cyclic nucleotide gated channel, plant\|(RefSeq) CNGC10; cyclic nucleotide gated channel 10 |
| AT2G04030 | 4334.291 | − 0.589 | 0.0000 | CR88 | K09487 heat shock protein 90 kDa beta\|(RefSeq) CR88; Chaperone protein htpG family protein |
| AT2G41090 | 10067.394 | − 0.576 | 0.0120 | AT2G41090 | K02183 calmodulin\|(RefSeq) Calcium-binding EF-hand family protein |
| AT2G46440 | 1746.229 | − 0.544 | 0.0000 | CNGC11 | K05391 cyclic nucleotide gated channel, plant\|(RefSeq) CNGC11; cyclic nucleotide-gated channels 11 |
| AT2G46450 | 2058.181 | − 0.487 | 0.0000 | CNGC12 | K05391 cyclic nucleotide gated channel, plant\|(RefSeq) CNGC12; cyclic nucleotide-gated channel 12 |
| AT5G45250 | 1325.331 | − 0.458 | 0.0002 | RPS4 | K16226 disease resistance protein RPS4\|(RefSeq) RPS4; Disease resistance protein (TIR-NBS-LRR class) family |
| AT5G54250 | 1415.940 | − 0.421 | 0.0005 | CNGC4 | K05391 cyclic nucleotide gated channel, plant\|(RefSeq) CNGC4; cyclic nucleotide-gated cation channel |
| AT4G02930 | 1628.546 | − 0.399 | 0.0208 | AT4G02930 | K02358 elongation factor Tu\|(RefSeq) GTP binding Elongation factor Tu family protein |
| AT3G25070 | 1129.607 | − 0.349 | 0.0096 | RIN4 | K13456 RPM1-interacting protein 4\|(RefSeq) RIN4; RPM1 interacting protein 4 |
| AT5G45260 | 839.522 | − 0.294 | 0.0243 | RRS1 | K16225 probable WRKY transcription factor 52\|(RefSeq) RRS1; Disease resistance protein (TIR-NBS-LRR class) family |
| AT2G41410 | 5202.793 | 0.330 | 0.0092 | AT2G41410 | K13448 calcium-binding protein CML\|(RefSeq) Calcium-binding EF-hand family protein |
| AT3G51850 | 1267.797 | 0.338 | 0.0001 | CPK13 | K13412 calcium-dependent protein kinase [EC:2.7.11.1]\|(RefSeq) CPK13; calcium-dependent protein kinase 13 |
| AT4G35310 | 3022.246 | 0.342 | 0.0049 | CPK5 | K13412 calcium-dependent protein kinase [EC:2.7.11.1]\|(RefSeq) CPK5; calmodulin-domain protein kinase 5 |
| AT1G18210 | 2013.900 | 0.401 | 0.0297 | AT1G18210 | K13448 calcium-binding protein CML\|(RefSeq) Calcium-binding EF-hand family protein |
| AT4G09570 | 699.429 | 0.432 | 0.0015 | CPK4 | K13412 calcium-dependent protein kinase [EC:2.7.11.1]\|(RefSeq) CPK4; calcium-dependent protein kinase 4 |
| AT5G23580 | 504.815 | 0.467 | 0.0209 | CDPK9 | K13412 calcium-dependent protein kinase [EC:2.7.11.1]\|(RefSeq) CDPK9; calmodulin-like domain protein 9 |
| AT1G07720 | 574.720 | 0.483 | 0.0277 | KCS3 | K15397 3-ketoacyl-CoA synthase [EC:2.3.1.199]\|(RefSeq) KCS3; 3-ketoacyl-CoA synthase 3 |
| AT2G30250 | 1510.606 | 0.515 | 0.0008 | WRKY25 | K13423 WRKY transcription factor 25\|(RefSeq) WRKY25; WRKY DNA-binding protein 25 |
| AT3G07040 | 441.852 | 0.515 | 0.0021 | RPM1 | K13457 disease resistance protein RPM1\|(RefSeq) RPM1; NB-ARC domain-containing disease resistance protein RPM1 |
| AT5G20480 | 435.555 | 0.518 | 0.0138 | EFR | K13428 LRR receptor-like serine/threonine-protein kinase EFR [EC:2.7.11.1]\|(RefSeq) EFR; LRR receptor-like serine/threonine-protein kinase |
| AT1G18890 | 845.571 | 0.520 | 0.0000 | CDPK1 | K13412 calcium-dependent protein kinase [EC:2.7.11.1]\|(RefSeq) CDPK1; calcium-dependent protein kinase 1 |
| AT5G53130 | 1629.894 | 0.588 | 0.0000 | CNGC1 | K05391 cyclic nucleotide gated channel, plant\|(RefSeq) CNGC1; cyclic nucleotide gated channel 1 |
| AT5G43760 | 1663.401 | 0.589 | 0.0003 | KCS20 | K15397 3-ketoacyl-CoA synthase [EC:2.3.1.199]\|(RefSeq) KCS20; 3-ketoacyl-CoA synthase 20 |
| AT3G28910 | 406.965 | 0.606 | 0.0475 | MYB30 | K23865 transcription factor MYB30\|(RefSeq) MYB30; myb domain protein 30 |
| AT3G51920 | 2068.519 | 0.607 | 0.0000 | CAM9 | K13448 calcium-binding protein CML\|(RefSeq) CAM9; calmodulin 9 |
| AT4G21940 | 197.382 | 0.627 | 0.0001 | CPK15 | K13412 calcium-dependent protein kinase [EC:2.7.11.1]\|(RefSeq) CPK15; calcium-dependent protein kinase 15 |
| AT2G17290 | 1424.447 | 0.629 | 0.0000 | CPK6 | K13412 calcium-dependent protein kinase [EC:2.7.11.1]\|(RefSeq) CPK6; Calcium-dependent protein kinase 6 |
| AT4G30560 | 143.601 | 0.632 | 0.0025 | CNGC9 | K05391 cyclic nucleotide gated channel, plant\|(RefSeq) CNGC9; cyclic nucleotide gated channel 9 |
| AT2G13790 | 1560.665 | 0.634 | 0.0052 | SERK4 | K13417 somatic embryogenesis receptor kinase 4 [EC:2.7.10.1 2.7.11.1]\|(RefSeq) SERK4; somatic embrio |
| AT1G64060 | 863.281 | 0.646 | 0.0314 | RBOH_F | K13447 respiratory burst oxidase [EC:1.6.3.- 1.11.1.-]\|(RefSeq) RBOH_F; respiratory burst oxidase |
| AT5G49480 | 594.435 | 0.681 | 0.0009 | CP1 | K02183 calmodulin\|(RefSeq) CP1; Ca2 + -binding protein 1 |
| AT4G08500 | 1522.429 | 0.727 | 0.0000 | MEKK1 | K13414 mitogen-activated protein kinase kinase kinase 1 [EC:2.7.11.25]\|(RefSeq) MEKK1; MAPK/ERK kinase |
| AT5G04870 | 1428.106 | 0.788 | 0.0000 | CPK1 | K13412 calcium-dependent protein kinase [EC:2.7.11.1]\|(RefSeq) CPK1; calcium dependent protein kinase |
| AT5G47910 | 10418.931 | 0.813 | 0.0002 | RBOH_D | K13447 respiratory burst oxidase [EC:1.6.3.- 1.11.1.-]\|(RefSeq) RBOHD; respiratory burst oxidase h |
| AT3G21220 | 1027.608 | 0.857 | 0.0000 | MKK5 | K13413 mitogen-activated protein kinase kinase 4/5 [EC:2.7.12.2]\|(RefSeq) MKK5; MAP kinase kinase |
| AT5G56580 | 73.090 | 0.909 | 0.0002 | MKK6 | K04368 mitogen-activated protein kinase kinase 1 [EC:2.7.12.2]\|(RefSeq) MKK6; MAP kinase kinase 6 |
| AT3G50770 | 2199.618 | 0.915 | 0.0020 | CML41 | K13448 calcium-binding protein CML\|(RefSeq) CML41; calmodulin-like 41 |
| AT3G48090 | 1138.791 | 0.960 | 0.0000 | EDS1 | K18875 enhanced disease susceptibility 1 protein\|(RefSeq) EDS1; alpha/beta-hydrolases superfamily |
| AT1G04220 | 43.059 | 0.974 | 0.0359 | KCS2 | K15397 3-ketoacyl-CoA synthase [EC:2.3.1.199]\|(RefSeq) KCS2; 3-ketoacyl-CoA synthase 2 |
| AT1G21550 | 353.248 | 0.985 | 0.0034 | CML44 | K13448 calcium-binding protein CML\|(RefSeq) Calcium-binding EF-hand family protein |
| AT3G10300 | 2515.275 | 1.046 | 0.0000 | CML49 | K13448 calcium-binding protein CML\|(RefSeq) Calcium-binding EF-hand family protein |
| AT2G43230 | 17.317 | 1.078 | 0.0388 | CARK6 | K13436 pto-interacting protein 1 [EC:2.7.11.1]\|(RefSeq) Protein kinase superfamily protein |
| AT3G25600 | 701.829 | 1.083 | 0.0000 | CML16 | K13448 calcium-binding protein CML\|(RefSeq) Calcium-binding EF-hand family protein |
| AT2G41110 | 334.904 | 1.090 | 0.0000 | CAM2 | K02183 calmodulin\|(RefSeq) CAM2; calmodulin 2 |
| AT3G59350 | 3517.027 | 1.115 | 0.0000 | CARK5 | K13436 pto-interacting protein 1 [EC:2.7.11.1]\|(RefSeq) Protein kinase superfamily protein |
| AT2G47060 | 1503.039 | 1.182 | 0.0000 | PTI1-4 (syn. CARK3) | K13436 pto-interacting protein 1 [EC:2.7.11.1]\|(RefSeq) PTI1-4; Protein kinase superfamily protein |

Continued

| Gene ID | baseMean | log2FoldChange | $p_{adj}$ | Gene symbol | KEGG\|NCBI Refseq description |
|---|---|---|---|---|---|
| AT3G45640 | 9125.245 | 1.195 | 0.0000 | MPK3 | K20536 mitogen-activated protein kinase 3 [EC:2.7.11.24]\|(RefSeq) MPK3; mitogen-activated protein |
| AT2G38470 | 9117.658 | 1.299 | 0.0000 | WRKY33 | K13424 WRKY transcription factor 33\|(RefSeq) WRKY33; WRKY DNA-binding protein 33 |
| AT2G24610 | 13.558 | 1.356 | 0.0042 | CNGC14 | K05391 cyclic nucleotide gated channel, plant\|(RefSeq) CNGC14; cyclic nucleotide-gated channel 14 |
| AT1G01120 | 615.654 | 1.369 | 0.0000 | KCS1 | K15397 3-ketoacyl-CoA synthase [EC:2.3.1.199]\|(RefSeq) KCS1; 3-ketoacyl-CoA synthase 1 |
| AT1G66400 | 142.657 | 1.379 | 0.0000 | CML23 | K13448 calcium-binding protein CML\|(RefSeq) CML23; calmodulin like 23 |
| AT3G25250 | 127.057 | 1.4102 | 0.0000 | AGC2-1 (syn. OXI1) | K20714 AGC2, AGC2 kinase 1, AtOXI1, OXI1, oxidative signal-inducible1 \|(RefSeq) AGC (cAMP-dependent, cGMP-dependent and protein kinase C) kinase family protein |
| AT2G41100 | 6876.659 | 1.485 | 0.0000 | TCH3 | K13448 calcium-binding protein CML\|(RefSeq) TCH3; Calcium-binding EF hand family protein |
| AT3G57530 | 4841.307 | 1.574 | 0.0000 | CPK32 | K13412 calcium-dependent protein kinase [EC:2.7.11.1]\|(RefSeq) CPK32; calcium-dependent protein ki |
| AT4G01250 | 351.402 | 1.706 | 0.0000 | WRKY 22 | K13425 WRKY transcription factor 22\|(RefSeq) WRKY22; WRKY family transcription factor |
| AT5G37770 | 2106.314 | 1.774 | 0.0000 | TCH2 | K13448 calcium-binding protein CML\|(RefSeq) TCH2; EF hand calcium-binding protein family |
| AT3G17690 | 182.335 | 1.854 | 0.0000 | CNGC19 | K05391 cyclic nucleotide gated channel, plant\|(RefSeq) CNGC19; cyclic nucleotide gated channel 19 |
| AT1G76040 | 1268.937 | 1.877 | 0.0000 | CPK29 | K13412 calcium-dependent protein kinase [EC:2.7.11.1]\|(RefSeq) CPK29; calcium-dependent protein kinase |
| AT1G76650 | 3612.023 | 1.925 | 0.0000 | CML38 | K13448 calcium-binding protein CML\|(RefSeq) CML38; calmodulin-like 38 |
| AT2G43290 | 1726.019 | 1.950 | 0.0000 | MSS3 | K13448 calcium-binding protein CML\|(RefSeq) MSS3; Calcium-binding EF-hand family protein |
| AT5G66210 | 4849.403 | 1.999 | 0.0000 | CPK28 | K13412 calcium-dependent protein kinase [EC:2.7.11.1]\|(RefSeq) CPK28; calcium-dependent protein kinase |
| AT3G01830 | 435.539 | 2.035 | 0.0000 | CML40 | K13448 calcium-binding protein CML\|(RefSeq) Calcium-binding EF-hand family protein |
| AT5G42380 | 767.085 | 2.144 | 0.0000 | CML37 | K13448 calcium-binding protein CML\|(RefSeq) CML37; calmodulin like 37 |

**Table 1**. List of genes involved in calcium perception and signal transduction. Significantly differentially expressed genes were limited to the adjusted $p$-value < 0.05 ($p_{adj}$ < 0.05).

proteins are products of genes expressed in the leaf vasculature and constitutively up-regulated in *Atseor1ko* mutants.

Theoretically, the $Ca^{2+}$ binding domain of AtSEOR2 may serve to withdraw $Ca^{2+}$ by competition from other $Ca^{2+}$ binding proteins. In the light of the phytoplasma-induced elevation of the intracellular $Ca^{2+}$ level in SE, however, it is more likely that $Ca^{2+}$- transformed AtSEOR2 is able to activate other proteins (e. g. CAM2, TCH3, CML49) with or without the delivery of $Ca^{2+}$ ions. These proteins may be involved in the regulation of gene clusters that shape a platform controlling and directing nutrient investments in growth and defense. Up-regulation of genes stimulated by AtSEOR2 would drive the plant metabolism in the direction of defense investment, while AtSEOR2-mediated downregulation of other genes would limit nutrient investment in growth. In accordance with this concept, phytoplasma effectors are expected to interfere with the stimulation of defense genes and propel the plant metabolism towards investment in growth.

## $SAP54_{CY}$ and AtSEOR2 both possess a structure interactive with the calcium-binding EF hand family protein TCH3

As initial attempt to test the validity of the previous hypothesis, a potential interaction between the phytoplasma effector $SAP54_{CY}$ and protein actors in the defense/growth regulatory platform was investigated. So far, the action of $SAP54_{CY}$ provides credence for this concept. It is well known that bacterial effectors can co-opt, directly or indirectly, host calmodulins to inhibit immunity[60]. So, in phytoplasma-infected wild-type plants, $SAP54_{CY}$ can use SOC1 as a co-factor to interact with TCH3 protein to boost plant vegetative growth and simultaneously suppress TCH3-mediated plant resistance[61–63]. In infected *Atseor1ko* plants, AtSEOR2 protein can interact with TCH3, to promote TCH3 cooperation with other calcium-sensor proteins to trigger plant immune response[34], thus competing with $SAP54_{CY}$ to have an implicit control on plant growth and development.

## Concluding remarks

As a final conclusion, AtSEOR2 seems to effect on a regulatory platform that controls the nutrition investment between growth and defense efforts in an unknown fashion. AtSEOR2 stimulates the defense efforts and is counteracted by effectors as, for instance, the plant growth-stimulating $SAP54_{CY}$. It should be noted that AtSEOR2 is a multitasker (Fig. 8). In healthy wild-type plants, AtSEOR2 is probably mostly in the unbound form, prepared to action. When the $Ca^{2+}$ level rises in SEs due to infection, part of the $Ca^{2+}$ will be used for a fusion between AtSEOR2 and AtSEOR1 to create sieve-pore plugs (Fig. 8). A portion of the $Ca^{2+}$ content may bind to free AtSEOR2, but the amount of free AtSEOR2 may be appreciably lower than in mutant plants. The response of the SEOR proteins to $Ca^{2+}$ might not be universal among higher plants, as reported by Mullendore et al.[64] in *Populus trichocarpa*. This species possesses non-dispersive protein bodies that contain a unique protein encoded by a gene annotated as a homolog of AtSEOR1.

In contrast to several other proteins, SEOR production may be completed during the final stage of SE ontogenesis[65]. This would imply that SEOR2 production is not further sustained by turn-over supply from the companion cells (CCs). How changes in SEs associated with phytoplasma infection are communicated to CCs

| Gene ID | baseMean | log2FoldChange | $p_{adj}$ | Gene symbol | KEGG\|NCBI Refseq description |
|---|---|---|---|---|---|
| AT3G16360 | 92.533 | − 1.425 | 0.0031 | AHP4 | K14490 histidine-containing phosphotransfer peotein\|(RefSeq) AHP4; HPT phosphotransmitter 4 |
| AT1G48500 | 69.546 | − 1.048 | 0.0502 | JAZ4 | K13464 jasmonate ZIM domain-containing protein\|(RefSeq) JAZ4; jasmonate-ZIM-domain protein 4 |
| AT4G36110 | 89.645 | − 0.952 | 0.0458 | SAUR9 | K14488 SAUR family protein\|(RefSeq) SAUR9; SAUR-like auxin-responsive protein family |
| AT1G77920 | 1094.475 | − 0.814 | 0.0036 | TGA7 | K14431 transcription factor TGA\|(RefSeq) TGA7; bZIP transcription factor family protein |
| AT2G36270 | 258.037 | − 0.745 | 0.0013 | ABI5 | K14432 ABA responsive element binding factor \|(RefSeq) ABI5; Basic-leucine zipper (bZIP) transcription factor |
| AT3G50750 | 813.505 | − 0.539 | 0.0013 | BEH1 | K14503 brassinosteroid resistant 1/2\|(RefSeq) BEH1; BES1/BZR1 homolog 1 |
| AT5G42750 | 357.417 | − 0.516 | 0.0010 | BKI1 | K14499 BRI1 kinase inhibitor 1\|(RefSeq) BKI1; BRI1 kinase inhibitor 1 |
| AT5G25350 | 1015.707 | − 0.477 | 0.0473 | EBF2 | K14515 EIN3-binding F-box protein\|(RefSeq) EBF2; EIN3-binding F box protein 2 |
| AT1G60940 | 1759.825 | − 0.378 | 0.0028 | SNRK2.10 | K14498 serine/threonine-protein kinase SRK2 [EC:2.7.11.1] \|(RefSeq) SNRK2.10; SNF1-related protein |
| AT2G40940 | 1262.022 | − 0.355 | 0.0192 | ERS1 | K14509 ethylene receptor [EC:2.7.13.-]\|(RefSeq) ERS1; ethylene response sensor 1 |
| AT5G27320 | 509.788 | − 0.290 | 0.0455 | GID1C | K14493 gibberellin receptor GID1 [EC:3.-.-.-]\|(RefSeq) GID1C; alpha/beta-hydrolases superfamily protein |
| AT5G41260 | 2229.433 | − 0.282 | 0.0209 | BSK8 | K14500 BR-signaling kinase [EC:2.7.11.1]\|(RefSeq) BSK8; kinase with tetratricopeptide repeat domain |
| AT5G03730 | 1741.075 | − 0.252 | 0.0463 | CTR1 | K14510 serine/threonine-protein kinase CTR1 [EC:2.7.11.1]\|(RefSeq) CTR1; Protein kinase superfamily |
| AT2G39940 | 1025.463 | − 0.248 | 0.0301 | COI1 | K13463 coronatine-insensitive protein 1\|(RefSeq) COI1; RNI-like superfamily protein |
| AT3G29350 | 695.941 | 0.246 | 0.0416 | AHP2 | K14490 histidine-containing phosphotransfer peotein\|(RefSeq) AHP2; histidine-containing phosphotranferase peotein |
| AT2G25490 | 4286.714 | 0.312 | 0.0344 | EBF1 | K14515 EIN3-binding F-box protein\|(RefSeq) EBF1; EIN3-binding F box protein 1 |
| AT1G04550 | 445.063 | 0.337 | 0.0270 | IAA12 | K14484 auxin-responsive protein IAA\|(RefSeq) IAA12; AUX/IAA transcriptional regulator family protein |
| AT5G47220 | 2676.626 | 0.381 | 0.0296 | ERF2 | K14517 ethylene-responsive transcription factor 2\|(RefSeq) ERF2; ethylene responsive element binding |
| AT1G64280 | 1342.858 | 0.395 | 0.0047 | NPR1 | K14508 regulatory protein NPR1\|(RefSeq) NPR1; regulatory protein (NPR1) |
| AT5G59220 | 417.598 | 0.572 | 0.0475 | HAI1 | K14497 protein phosphatase 2C [EC:3.1.3.16]\|(RefSeq) HAI1; PP2C protein (Clade A protein phosphatase) |
| AT3G61830 | 428.868 | 0.609 | 0.0249 | ARF18 | K14486 auxin response factor\|(RefSeq) ARF18; auxin response factor 18 |
| AT3G50070 | 181.632 | 0.621 | 0.0317 | CYCD3;3 | K14505 cyclin D3, plant\|(RefSeq) CYCD3;3; CYCLIN D3;3 |
| AT3G17860 | 1131.169 | 0.629 | 0.0001 | JAZ3 | K13464 jasmonate ZIM domain-containing protein\|(RefSeq) JAZ3; jasmonate-ZIM-domain protein 3 |
| AT1G51950 | 997.557 | 0.635 | 0.0000 | IAA18 | K14484 auxin-responsive protein IAA\|(RefSeq) IAA18; indole-3-acetic acid inducible 18 |
| AT2G22670 | 2341.781 | 0.643 | 0.0002 | IAA8 | K14484 auxin-responsive protein IAA\|(RefSeq) IAA8; indoleacetic acid-induced protein 8 |
| AT2G38120 | 1492.354 | 0.736 | 0.0096 | AUX1 | K13946 auxin influx carrier (AUX1 LAX family)\|(RefSeq) AUX1; Transmembrane amino acid transporter |
| AT1G19850 | 648.147 | 0.741 | 0.0049 | MP | K14486 auxin response factor\|(RefSeq) MP; Transcriptional factor B3 family protein / auxin-response factor |
| AT2G21050 | 560.594 | 0.744 | 0.0297 | LAX2 | K13946 auxin influx carrier (AUX1 LAX family)\|(RefSeq) LAX2; uncharacterized protein |
| AT5G54510 | 514.212 | 0.775 | 0.0054 | DFL1 | K14487 auxin responsive GH3 gene family\|(RefSeq) DFL1; Auxin-responsive GH3 family protein |
| AT5G13220 | 3618.217 | 0.806 | 0.0502 | JAZ10 | K13464 jasmonate ZIM domain-containing protein\|(RefSeq) JAZ10; jasmonate-ZIM-domain protein 10 |
| AT3G57040 | 270.797 | 0.842 | 0.0243 | ARR9 | K14492 two-component response regulator ARR-A family\|(RefSeq) ARR9; response regulator 9 |
| AT1G10470 | 1629.885 | 0.844 | 0.0006 | ARR4 | K14492 two-component response regulator ARR-A family\|(RefSeq) ARR4; response regulator 4 |
| AT3G21220 | 1027.608 | 0.857 | 0.0000 | MKK5 | K13413 mitogen-activated protein kinase kinase 4/5 [EC:2.7.12.2]\|(RefSeq) MKK5; MAP kinase kinase |
| AT4G34160 | 462.702 | 0.892 | 0.0000 | CYCD3;1 | K14505 cyclin D3, plant\|(RefSeq) CYCD3;1; CYCLIN D3;1 |
| AT5G53590 | 471.312 | 0.925 | 0.0007 | AT5G53590 | K14488 SAUR family protein\|(RefSeq) SAUR-like auxin-responsive protein family |
| AT5G50760 | 56.915 | 0.961 | 0.0433 | AT5G50760 | K14488 SAUR family protein\|(RefSeq) SAUR-like auxin-responsive protein family |
| AT4G27260 | 699.893 | 0.964 | 0.0000 | WES1 | K14487 auxin responsive GH3 gene family\|(RefSeq) WES1; Auxin-responsive GH3 family protein |
| AT2G01830 | 522.585 | 0.981 | 0.0007 | WOL | K14489 *Arabidopsis* histidine kinase 2/3/4 (cytokinin receptor) EC:2.7.13.3]\|(RefSeq) WOL; CHASE d |
| AT5G13320 | 844.274 | 1.028 | 0.0094 | PBS3 | K14487 auxin responsive GH3 gene family\|(RefSeq) PBS3; Auxin-responsive GH3 family protein |
| AT4G22620 | 7.880 | 1.126 | 0.0380 | AT4G22620 | K14488 SAUR family protein\|(RefSeq) SAUR-like auxin-responsive protein family |
| AT1G19050 | 405.434 | 1.128 | 0.0002 | ARR7 | K14492 two-component response regulator ARR-A family\| (RefSeq) ARR7; response regulator 7 |
| AT3G62100 | 19.865 | 1.154 | 0.0097 | IAA30 | K14484 auxin-responsive protein IAA\|(RefSeq) IAA30; indole-3-acetic acid inducible 30 |
| AT4G12410 | 20.058 | 1.193 | 0.0070 | AT4G12410 | K14488 SAUR family protein\|(RefSeq) SAUR-like auxin-responsive protein family |
| AT2G14960 | 6.773 | 1.226 | 0.0235 | GH3.1 | K14487 auxin responsive GH3 gene family\|(RefSeq) GH3.1; Auxin-responsive GH3 family protein |
| AT3G15540 | 162.008 | 1.266 | 0.0000 | IAA19 | K14484 auxin-responsive protein IAA\|(RefSeq) IAA19; indole-3-acetic acid inducible 19 |
| AT1G17380 | 4677.462 | 1.357 | 0.0000 | JAZ5 | K13464 jasmonate ZIM domain-containing protein\|(RefSeq) JAZ5; jasmonate-ZIM-domain protein 5 |
| AT1G19180 | 7445.883 | 1.491 | 0.0000 | JAZ1 | K13464 jasmonate ZIM domain-containing protein\|(RefSeq) JAZ1; jasmonate-ZIM-domain protein 1 |
| AT4G11280 | 2993.356 | 1.6125 | 0.000 | ACS6 | K20772 1-aminocyclopropane-1-carboxylic acid (acc) synthase 6, ATACS6, F8L21.70, F8L21_70 \|(RefSeq) ACS6; 1-aminocyclopropane-1-carboxylic acid (acc) synthase 6 |
| AT5G45110 | 3227.671 | 1.724 | 0.0000 | NPR3 | K14508 regulatory protein NPR1\|(RefSeq) NPR3; NPR1-like protein 3 |
| AT1G52830 | 25.583 | 1.966 | 0.0000 | IAA6 | K14484 auxin-responsive protein IAA\|(RefSeq) IAA6; indole-3-acetic acid 6 |
| Continued | | | | | |

| Gene ID | baseMean | log2FoldChange | $p_{adj}$ | Gene symbol | KEGG\|NCBI Refseq description |
|---|---|---|---|---|---|
| AT5G57560 | 5913.105 | 2.228 | 0.0000 | TCH4 | K14504 xyloglucan:xyloglucosyl transferase TCH4 [EC:2.4.1.207]\|(RefSeq) TCH4; Xyloglucan endotransferase |
| AT3G48100 | 524.7245 | 2.368 | 0.0000 | ARR5 | K14492 two-component response regulator ARR-A family\|(RefSeq) RR5; response regulator 5 |
| AT3G09870 | 26.685 | 2.974 | 0.0000 | SAUR48 | K14488 SAUR family protein\|(RefSeq) SAUR-like auxin responsive protein family |

**Table 2**. List of genes involved in phytohormone signal transduction. Significantly differentially expressed genes were limited to the adjusted $p$-value < 0.05 ($p_{adj}$ < 0.05).

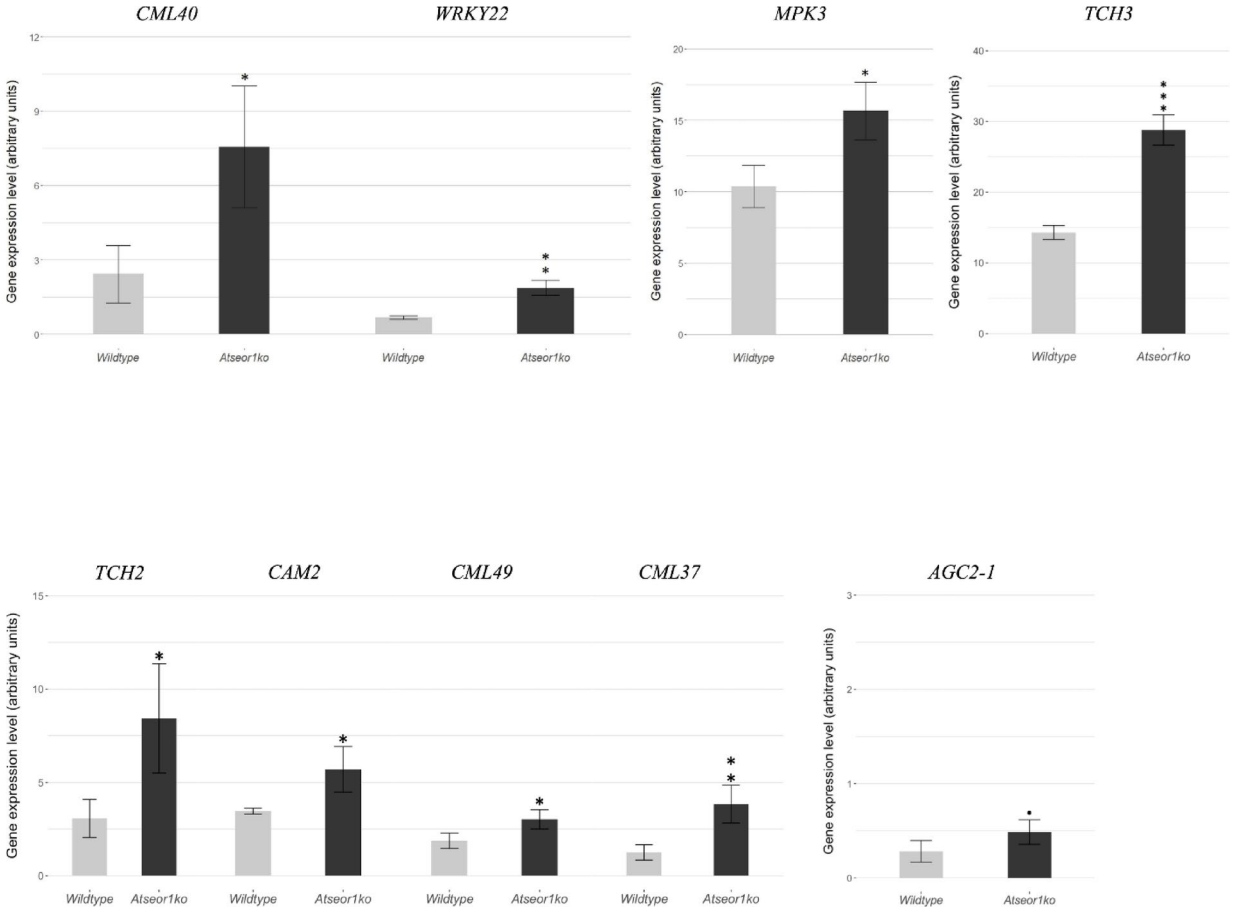


**Fig. 4**. Relative expression level of genes encoding proteins related to calcium signaling and encoding the WRKY22 transcription factor in the rosette leaves of healthy plants of wild-type and *Atseor1* mutant lines. Expression values were normalized to the UBC9 transcript level, arbitrarily fixed at 100, then expressed as the gene expression level. Statistical analyses were performed using an unpaired t-test. Family-wise significance and confidence level = 0.10 (• $0.10 > p > 0.05$, * $p < 0.05$, ** $p < 0.01$, *** $p < 0.001$, n.s.: not significant).

and beyond should be subject of subsequent studies. For a start, measurements of $Ca^{2+}$ changes in the respective intracellular compartments of SE/CCs and adjacent cells in the *Atseor1ko* line are required.

## Materials and methods

### Plant growth conditions

*Arabidopsis thaliana* lines used in this study had a Columbia (Col-0) background. Seeds of *AtSEOR1* knockout mutants (SALK_081968C), named *Atseor1ko* here, were obtained from the Nottingham *Arabidopsis* Stock Centre (NASC). Ten wild type and 10 *Atseor1ko* plants were grown at 20/22 °C under short-day conditions (9 h L/15 h D, light intensity 150–200 µmol/s/$m^2$). Prior to experiments, plants were cultivated for 72 days on a 5:1 mixture of soil substrate and perlite and fertilized twice a month with an N–P–K liquid fertilizer[11].

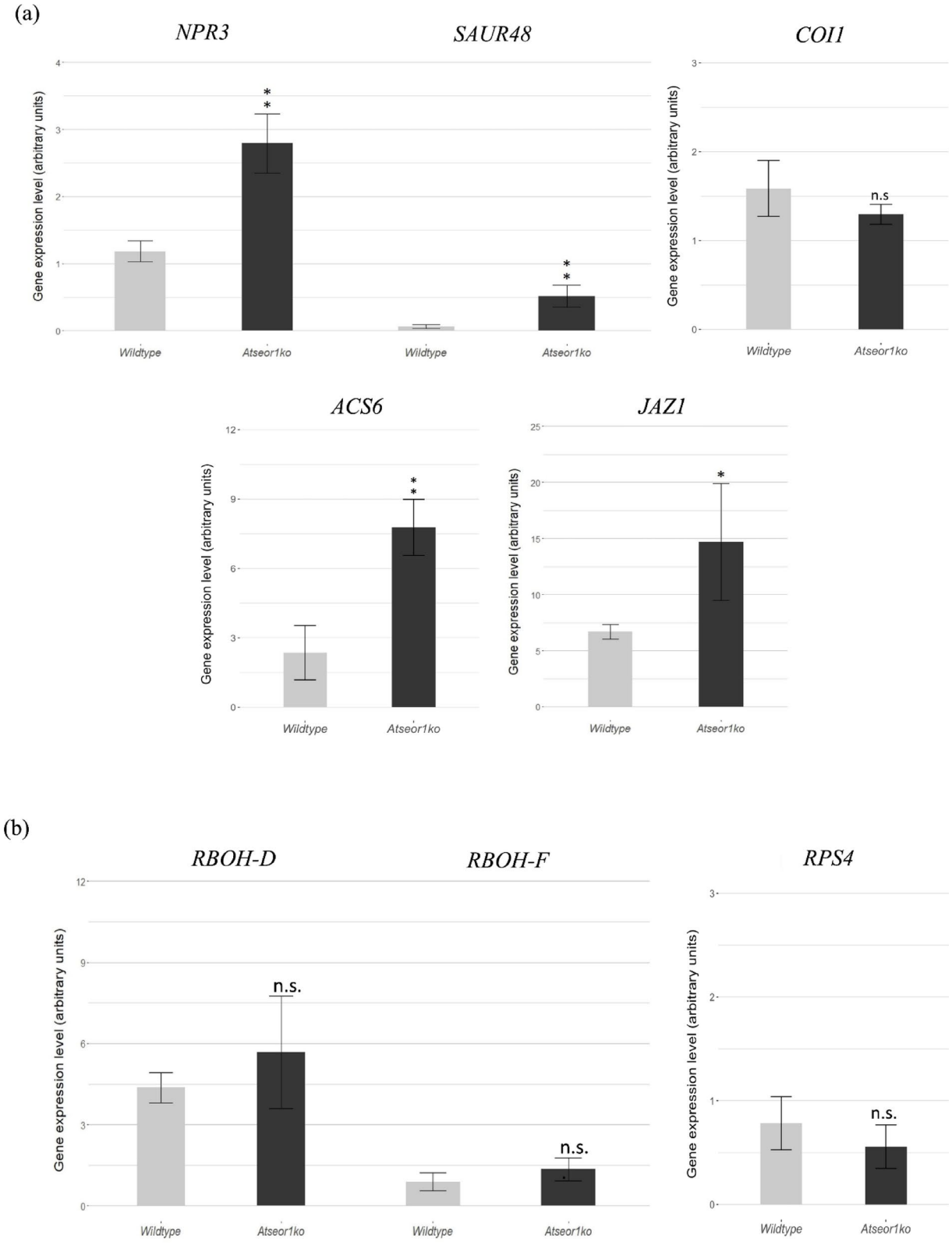


**Fig. 5**. Relative expression level of genes related to (**A**) hormone pathway and signaling and (**B**) plant defense, in the rosette leaves of healthy plants of wild-type and *Atseor1* mutant lines. Expression values were normalized to the UBC9 transcript level, arbitrarily fixed at 100, then expressed as the gene expression level. Statistical analyses were performed using an unpaired t-test. Family-wise significance and confidence level = 0.10 (• $0.10 > p > 0{,}05$, * $p < 0.05$, ** $p < 0.01$, *** $p < 0.001$, n.s.: not significant).

## RNA extraction, sequencing and bioinformatics analysis

Seventy-two-days-old plants were used for RNA-seq experiments. RNA was extracted from the leaf rosette, using the Spectrum Plant Total RNA kit (SigmaAldrich—Merck) following the manufacturer's instructions. Total RNA quantity and quality were analyzed with a Qubit RNA Br Assay kit (Thermo Fisher) after DNase treatment (Turbo DNA-free, Thermo Fisher). For all samples, the RNA integrity number (RIN) was greater than 7. Five biological replicates (plants) were analyzed for each line. Libraries were prepared from total RNA with an Illumina Stranded mRNA Prep Kit (Illumina Inc., San Diego, CA, USA), at the CRIBI NGS Facility (University of Padova, Italy). Libraries were sequenced on a NovaSeq 6000 Illumina platform as 100 bp paired-end stranded reads. For each library, more than 20 million reads were obtained and aligned to 32,832 genes. High-quality reads were deposited at the NCBI SRA database under BioProject ID: PRJNA1175435. Galaxy web server (https://usegalaxy.eu/, accessed on 5 January 2023) was used to perform differential gene expression analysis. FastQ files were uploaded to Galaxy and FASTQC was used to evaluate the quality of reads. The trimmomatic program was used to remove low-quality sequences and adapter sequences from the data. To ensure the minimum quality value of the reads, the cut-off value was set to 20 nucleotides. HISAT2 was used to align reads to the reference genome of *A. thaliana* Col-0. RNA STAR (Spliced Transcript Alignment to a Reference) was used to validate the output of HISAT2 alignment. Frequency of reads per gene was determined by the aid of featureCounts[66]. DESeq2 was used to normalize and display differential gene expression. Significantly DEGs were limited to the adjusted $p$-value < 0.05 ($p_{adj}$ < 0.05) and absolute fold change FC ≥ 2. To determine gene function both PANTHER (Protein Analysis THrough Evolutionary Relationships, https://www.pantherdb.org/) accessed on 7 January 2023, and GORILLA (Gene Ontology enRIchment anaLysis and visuaLizAtion tool, https://cbl-gorilla.cs.technion.ac.il/) accessed on 9 January 2023, classification systems were used. Differentially expressed genes (DEGs) were classified according to the Gene Ontology (GO) classification and the Kyoto Encyclopedia of Genes and Genomes [KEGG,[19]] pathway analysis.

## Gene expression analysis via Reverse Transcriptase-quantitative PCR (RT-qPCR)

To validate RNA-seq data, the expression levels of 17 genes (Supplementary Table 1), relevant in this frame, because they are involved in calcium and phytohormone signaling pathways, were further analyzed by RT-qPCR. To this end, we analyzed the same RNA samples that were used for library construction and sequencing. Primers were designed to the *Arabidopsis* sequences as reported in the Supplementary Table 2. We quantified the expression of genes encoding, respectively, the calcium-binding calmodulin 2 (CAM2), calmodulin-like proteins (CML37, CML40, CML49), the touch proteins TCH2 (*syn.* CML24) and TCH3 (*syn.* CML12), the mitogen-activated protein kinase 3 (MPK3), the AGC (cAMP-dependent, cGMP-dependent and protein kinase C) protein kinase 2 (AGC2-1, *syn.* OXI1), the WRKY transcription factor 22 (WRKY 22), the small auxin upregulated RNA 48 (SAUR48), jasmonate-ZIM-domain protein 1 (JAZ1), the non-expressor of pathogenesis-related gene 1 (NPR1)-like protein 3 (NPR3), the resistant to *Pseudomonas syringae* protein 4 (RPS4), the respiratory burst oxidase protein D (RBOHD) and respiratory burst oxidase homolog F (RBOHF), the stress-responsive 1-aminocyclopropane-1-carboxylic acid synthase 6 (ACS6), and the JA pathway marker protein coronatine insensitive 1 (COI1). The reference gene, *ubiquitin conjugating enzyme 9* (*UBQ9*), was run together with the 17 selected genes for internal normalization. It has been shown to be the most stably expressed [gene-stability measure M = 0.43,[67]] among a set of four potential reference genes [*UBC9*, *TIP41* (TIP41-like family protein), *SAND* (SAND family protein), and *UBQ10* (polyubiquitin 10)] analyzed on both wild type and *Atseor1ko* mutant RNA samples in previous work by our research group[11]. Total RNA was extracted using the Spectrum Plant Total RNA kit as described above, and then treated with the RQ1 RNase-Free DNase kit (Promega). The cDNA was prepared from high quality RNA using ImProm-II Reverse Transcription System Kit (Promega) according to the manufacturer's protocol. Primers used in this study (Supplementary Table 2) were designed with the Primer-BLAST software (National Center for Biotechnology Information, NCBI) with default settings except for adjustment of melting temperature to range from 60 to 65 °C. Primer pair efficiency was evaluated on the standard curves of different dilutions of pooled cDNA[68], obtaining amplification efficiencies higher than 90%. The RT-qPCR was performed on the Rotor-Gene Q instrument (Qiagen) using the QuantiNova SYBR Green PCR kit (Qiagen) and the amount of cDNA obtained from 4 ng of RNA, in a total volume of 20 µl. The PCR protocol included the following thermocycling conditions: initial denaturation and activation of Taq polymerase 95 °C; 3 min, denaturation 95 °C; 5 s, annealing/extension 60 °C for 10 s, 40 cycles. Results were analyzed by using the Rotor-Gene 2.0.3.2 Software version (Qiagen Italia, Milan, Italy). The relative concentration of each sample, compared to the reference sample, was calculated based on the takeoff point and amplification efficiency. The relative concentration, as calculated by the software, corresponds to: amplification efficiency^(takeoff of reference gene – takeoff of gene of interest). The relative concentration is expressed in arbitrary units (A. U.), calculated by normalizing the target gene to the reference gene, whose expression level is set to 100. Statistical analyses of gene expression levels were performed with R-Studio software (4.3.1) using an unpaired t-test.

## Infected plant material

For molecular analysis of infected plants, wild type and *Atseor1ko* plants were infested with *Euscelidius variegatus* as a phytoplasma vector ([11] and references herein). Healthy colonies of *E. variegatus* were reared on *Avena sativa* in vented plexiglass cages at 20/22 °C, under short-day conditions (9 h L/15 h D). Fourth and fifth instar nymphs were transferred to *Chrysanthemum carinatum* plants infected with CY phytoplasma, a strain related to '*Candidatus* Phytoplasma asteris' ('*Ca*. P. asteris', 16SrI-B subgroup)[69] as the source of inoculum for a 7-days-phytoplasma acquisition-access period (AAP). After the AAP, these insects were placed again on *A. sativa* for the 35-days latency period (LP), after which they had become infectious. Forty-five-days-old *A. thaliana* plants *per* line were then each exposed to three infectious insects during a phytoplasma inoculation access period (IAP) of

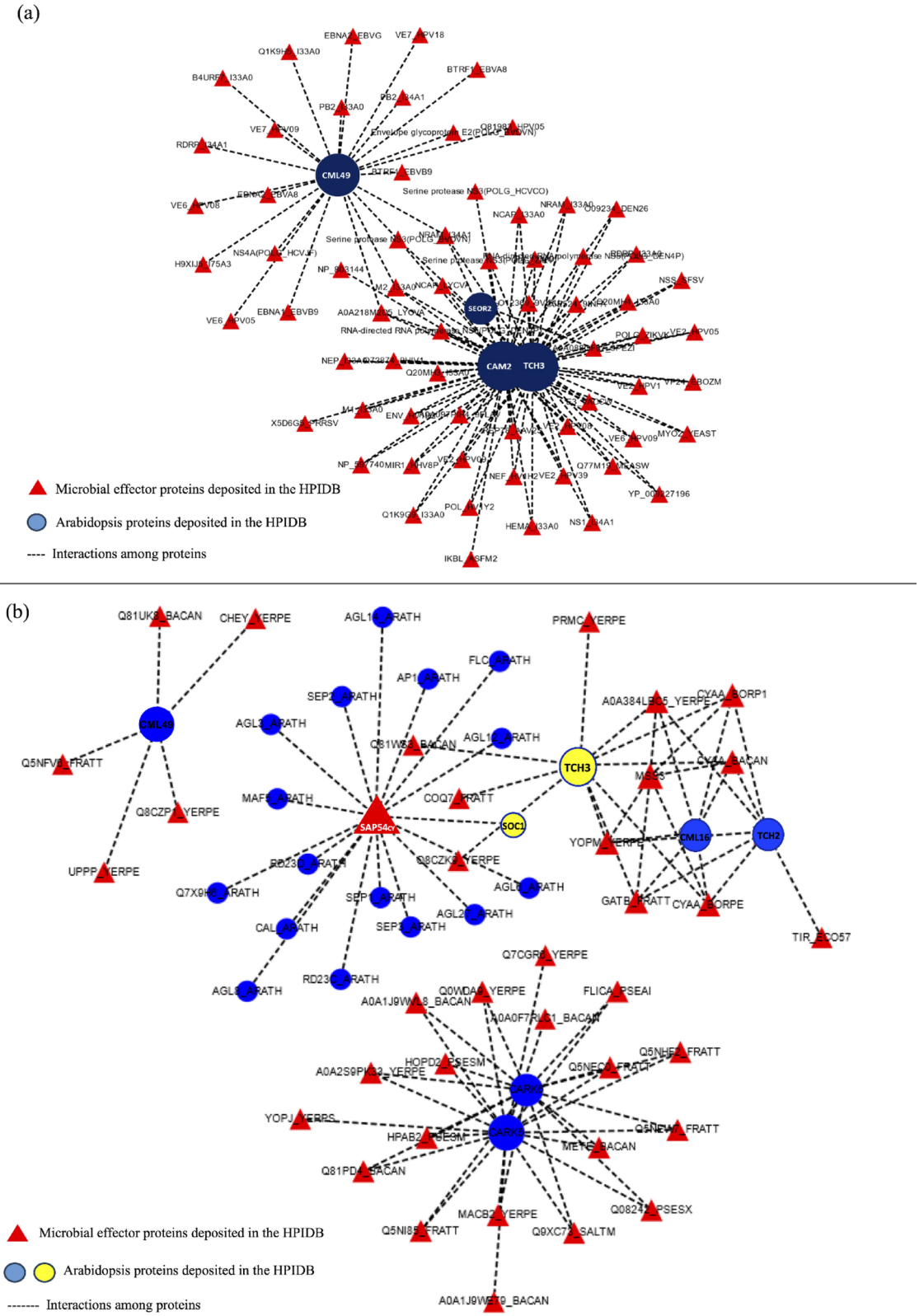


7 days, after which the insects were removed manually. Plants treated with three healthy leafhoppers, which were collected from healthy colonies and just as old as the infected ones, were used as a control.

## Phytoplasma detection in infected wild type and *Atseor1ko* plants and gene expression analysis of $SAP54_{CY}$ effector

To confirm the presence of CY phytoplasma in *Arabidopsis* lines treated with infectious insect vectors and determine the expression of the $SAP54_{CY}$ protein being a well characterized phytoplasma effector (Supplementary Fig. 1), we performed molecular analyses of leaf rosettes 20 days after IAP, when plants were 72 days old. Leaf

◀**Fig. 6**. Predicted interactions of *Arabidopsis* proteins with AtSEOR2 or SAP54$_{CY}$ effector. (**A**) Network analysis of interacting proteins encoded by the differentially expressed genes (DEGs) between *Atseor1ko* and wild type plants found in this study. Dark blue dots show *Arabidopsis* proteins predicted to interact with AtSEOR2 by HPIDB exploit. Interactions among proteins are depicted as dotted lines. Predicted interactions with other microbial effectors deposited in the database (red triangles) are also indicated. (**B**) Network analysis of proteins encoded by the DEGs found in this study and the SAP54$_{CY}$ effector. Blue and yellow dots mark *Arabidopsis* proteins predicted to interact with SAP54$_{CY}$ effector by HPIDB exploit. The yellow color is used to highlight the position of SOC1 and TCH3 proteins in the network. Interactions among proteins are depicted as dotted lines. Predicted interactions with other microbial effectors deposited in the database (red triangles) are also indicated.

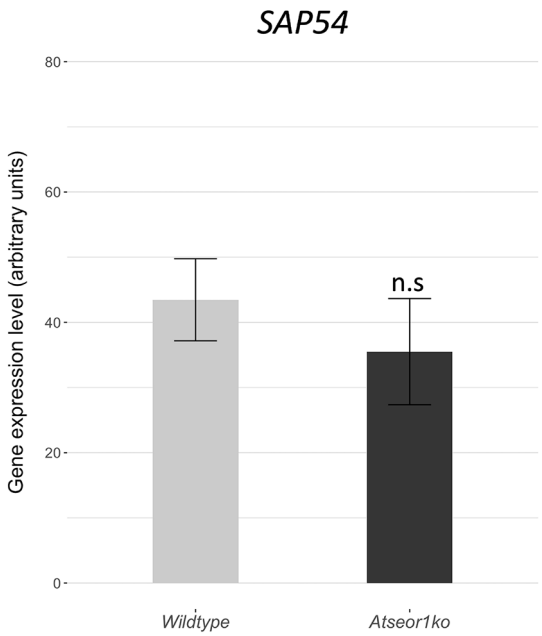


**Fig. 7**. Relative expression level of SAP54$_{CY}$ gene in the rosette leaves of CY-phytoplasma infected plants. Expression values were normalized to those of *dnaB, pykF* and *pfkA*, arbitrarily fixed at 100. The expression values were calculated by the geometric mean of the values obtained from normalization with each reference gene. Statistical analyses were performed using an unpaired t-test. Family-wise significance and confidence level = 0.10 (• $0{,}10 > p > 0{,}05$, * $p < 0.05$, ** $p < 0.01$, *** $p < 0.001$, n.s.: not significant).

rosettes were ground in a mortar with liquid nitrogen. RNA was then extracted and cDNA prepared as reported above. The ribosomal protein gene rpsC (rps3) was chosen as an indicator for amplification of CY phytoplasma cDNA (Supplementary Table 3),[70]. Specific primers designed for the CY phytoplasma genome by Pacifico et al.,[71] served to quantify the expression level of SAP54$_{CY}$ (Supplementary Tables 4 and 5). Gene expression was normalized to that of the reference genes DNA helicase B (*dnaB*), pyruvate kinase F (*pykF*) and ATP-dependent 6-phosphofructokinase A (*pfkA*) (Supplementary Table 5)[72,73].

The analyses were performed using three biological replicates with three technical replicates for each line (wild type and *Atseor1ko*) and conditions (infected and healthy). RT-qPCR analyses were executed on the Rotor-Gene Q instrument (Qiagen) by use of the QuantiNova SYBR Green PCR kit (Qiagen) and the amount of cDNA obtained from 15 ng of RNA, in a total volume of 20 µl. The PCR protocol included the following thermocycling conditions: initial denaturation and activation of Taq polymerase 95 °C; 3 min, denaturation 95 °C; 5 s, annealing/extension 56 °C for 10 s, 40 cycles. Amplification of the dilution series was carried out in order to calculate the primer pair efficiency of SAP54$_{CY}$ gene assay. Results were analyzed by the use of the Rotor-Gene 2.0.3.2 Software version (Qiagen Italia, Milan, Italy). The relative concentration of each sample, compared to the reference sample, was calculated based on the takeoff point and amplification efficiency. The relative concentration, as calculated by the software, corresponds to: amplification efficiency^(takeoff of reference gene – takeoff of gene of interest). The relative concentration is expressed in arbitrary units (A. U.), calculated by normalizing the target gene to the reference gene, whose expression level is set to 100. Expression values were calculated by the geometric mean of the values obtained from normalization with each reference gene[67]. Gene expression level was analyzed statistically by means of R-Studio software (4.3.1) using an unpaired t-test.

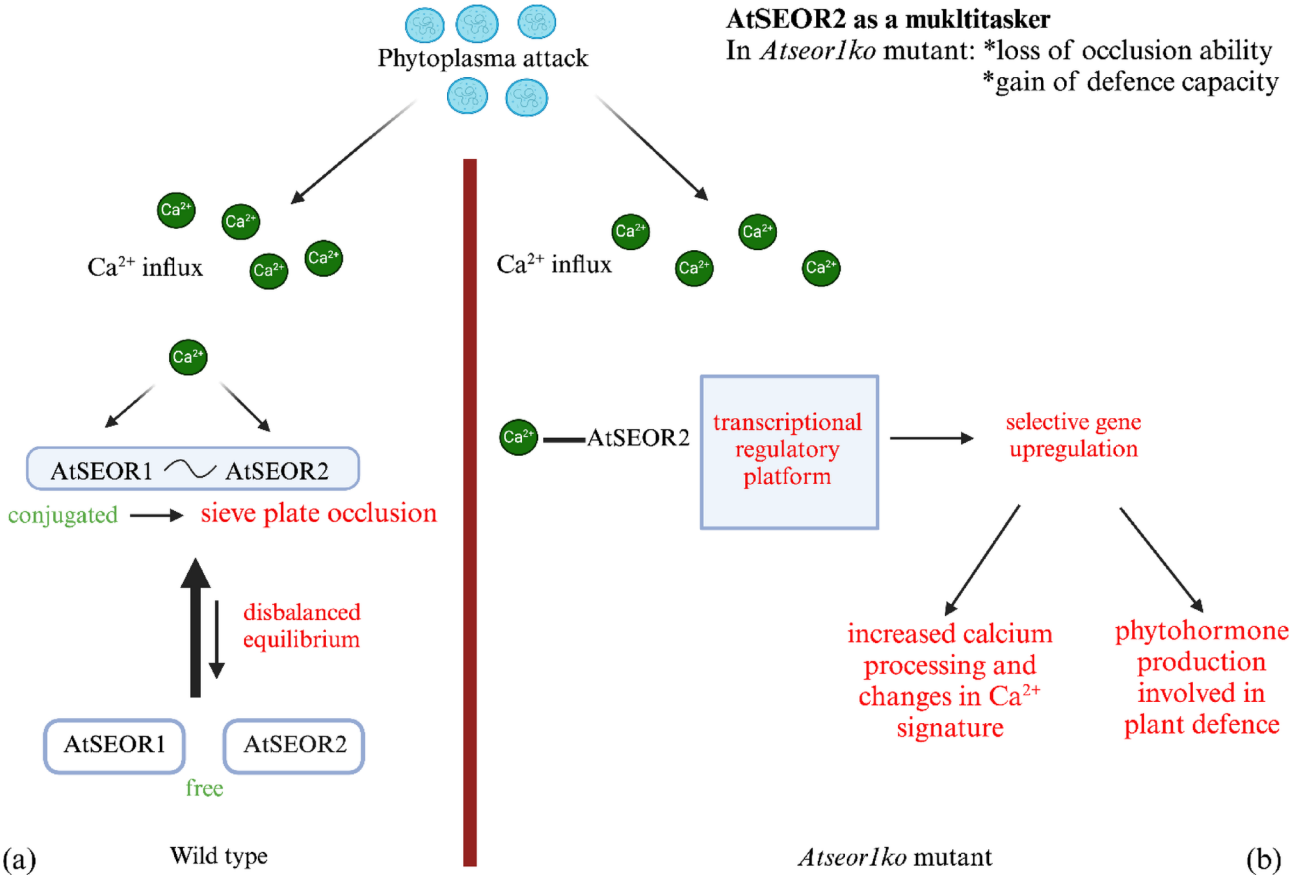


**Fig. 8**. A hypothetical model of overlapping multitasking by AtSEOR2 in the defense responses of *Arabidopsis* to phytoplasma infection. (**A**) Wild-type plants. Phytoplasma-induced elevation of the $Ca^{2+}$ level in sieve elements leads to a configuration change of free filamentous AtSEOR1 and AtSEOR2. $Ca^{2+}$-mediated AtSEOR1 ~ AtSEOR2 conjugation produces sieve-pore occluding plugs and thereby reduces the level of free AtSEORs to a likely considerable extent. Sieve-pore occlusion would affect the mobility of phytoplasmas. (**B**) *Atseor1ko* mutants. Phytoplasma-induced excess of $Ca^{2+}$ in sieve elements cannot be invested in the formation of AtSEOR-conjugates owing to the absence of AtSEOR1, but solely binds to AtSEOR2. Apparently, these $Ca^{2+}$-AtSEOR2 conjugates modulate a "transcriptional regulatory platform" to increase the expression of genes involved in defense-related $Ca^{2+}$ platform and genes that suppress plant growth. The platform is postulated to control the division of nutrient investment between defense and growth achievements. Phytoplasma effectors such as $SAP54_{CY}$ may interfere with the defensive efforts of AtSEOR2 via the common interaction hub TCH3.

## Detection of homology-based AtSEOR2 interaction networks

To display possible multiple interactions of AtSEOR2 with both the *Arabidopsis* proteins and the $SAP54_{CY}$ phytoplasma effector, the Host–Pathogen Interaction Data Base 3.0 (HPIDB 3.0),[20] was exploited. *A. thaliana*'s reference proteome (obtained from The *Arabidopsis* Information Resource, TAIR) was used to predict interactions of *Arabidopsis* proteins with $SAP54_{CY}$ effector, based on homology modeling[74,75], which is a well-established method to detect protein–protein interaction as reported by Koch et al.[76].

## Statistical analysis

For RNA-seq experiments, DESeq2 was used to normalize and display differential gene expression. Significantly DEGs were limited to the adjusted $p$-value < 0.05 ($p_{adj}$ < 0.05) and absolute fold change FC ≥ 2. For RNA-seq data validation via RT-qPCR, the same samples used for RNA-seq experiments were used, thus three wild-type and four *Atseor1ko* samples including three technical replicates each. Phytoplasma detection and *SAP54* expression analyses were performed using three infected and three healthy (control) individuals for each line, with three technical replicates each. The results were analyzed by using the Rotor-Gene 2.0.3.2 Software version (Qiagen Italia, Milan, Italy) and the data are expressed as average ± standard deviation (SD). Group comparisons were conducted using unpaired t-tests. Statistical analyses were performed using R software version 4.3.1 (R Core Team, Vienna, Austria). The significance was established at a two-tailed $p$-value of less than 0.05. Other information about the statistical analyses is provided in the figure legends.

## Data availability

The RNA-seq data generated in this study have been deposited in the NCBI SRA database under the accession code PRJNA1175435. The datasets used and/or analysed during the current study available from the corresponding author on reasonable request.

Received: 2 December 2024; Accepted: 6 May 2025
Published online: 22 May 2025

## References

1. van Bel, A. J. E. & Musetti, R. Sieve element biology provides leads for research on phytoplasma lifestyle in plant hosts. *J. Exp. Bot.* **70**, 3737–3755 (2019).
2. Shigetou, N. Molecular and biological properties of phytoplasmas. *Proc. Jpn. Acad. Ser. B Phys. Biol. Sci.* **95**(7), 401–418 (2019).
3. Duduk, B., Stepanović, J., Yadav, A. & Rao, G.P. Phytoplasmas in weeds and wild plants. In: Springer Nature Singapore Pte Ltd., Rao G.P. et al. (eds.), *Phytoplasmas: Plant Pathogenic Bacteria – I,* 313–345 (2018).
4. Zhang, J., Coaker, G., Zhou, J.-M. & Dong, X. Plant immune mechanisms from reductionistic to holistic points of view. *Mol. Plant* **13**, 1358–1378 (2020).
5. MacLean, A. M. et al. Phytoplasma effector SAP54 hijacks plant reproduction by degrading MADS-box proteins and promotes insect colonization in a RAD23-dependent manner. *PLoS Biol.* **12**, e1001835 (2014).
6. Huang, W. et al. Parasitic modulation of host development by ubiquitin-independent protein degradation. *Cell* **184**, 5201–5214 (2021).
7. Han, G.-Z. Origin and evolution of the plant immune system. *New Phytol.* **222**, 70–83 (2019).
8. Eveillard, S. et al. Contrasting susceptibilities to Flavescence Dorée in *Vitis vinifera*, rootstocks and wild *Vitis* species. *Front. Plant Sci.* **7**, 1762 (2016).
9. Seemüller, E. et al. Inheritance of apple proliferation resistance by parental lines of apomictic *Malus sieboldii* as donor of resistance in rootstock breeding. *Eur. J. Plant Pathol.* **151**, 767–779 (2018).
10. Casarin, S. et al. A successful defense strategy in grapevine cultivar "Tocai friulano" provides compartmentation of grapevine Flavescence dorée phytoplasma. *BMC Plant Biol.* **23**, 161 (2023).
11. Pagliari, L. et al. Filamentous sieve element proteins are able to limit phloem mass flow, but not phytoplasma spread. *J. Exp. Bot.* **68**, 3673–3688 (2017).
12. Bernardini, C. et al. Pre-symptomatic modified phytohormone profile is associated with lower phytoplasma titres in an *Arabidopsis seor1ko* line. *Sci. Rep.* **10**, 14770 (2020).
13. Anstead, J. A. et al. *Arabidopsis* P-protein filament formation requires both AtSEOR1 and AtSEOR2. *Plant Cell Physiol.* **53**, 1033–1042 (2012).
14. González-Fuente, M. et al. EffectorK, a comprehensive resource to mine for *Ralstonia, Xanthomonas,* and other published effector interactors in the *Arabidopsis* proteome. *Mol. Plant Pathol.* **21**, 1257–1270 (2020).
15. Arabidopsis Interactome Mapping Consortium. Evidence for network evolution in an *Arabidopsis* interactome map. *Science* **333**, 601–607 (2011).
16. Afzal, A. J., Kim, J. H. & Mackey, D. The role of NOI-domain containing proteins in plant immune signaling. *BMC Genom.* **14**, 327 (2013).
17. Daněk, M., Valentová, O. & Martinec, J. Flotillins, Erlins, and HIRs: From animal base camp to plant new horizons. *Crit. Rev. Plant Sci.* **35**, 191–214 (2016).
18. Pagliari, L., Buoso, S., Santi, S., van Bel, A. J. E. & Musetti, R. What slows down phytoplasma proliferation? Speculations on the involvement of AtSEOR2 protein in plant defense signalling. *Plant Signal. Behav.* **13**, e1473666 (2018).
19. Kanehisa, M., Furumichi, M., Sato, Y., Matsuura, Y. & Ishiguro-Watanabe, M. KEGG: Biological systems database as a model of the real world. *Nucleic Acids Res.* **53**, D672–D677. https://doi.org/10.1093/nar/gkae909 (2025).
20. Ammari, M. G., Gresham, C. R., McCarthy, F. M. & Nanduri, B. HPIDB 2.0: A curated database for host-pathogen interactions. *Database* **2016**, baw103 (2016).
21. Espadaler, J., Romero-Isart, O., Jackson, R. M. & Oliva, B. Prediction of protein–protein interactions using distant conservation of sequence patterns and structure relationships. *Bioinformatics* **21**, 3360–3368 (2005).
22. Knoblauch, M., Peters, W. S., Ehlers, K. & van Bel, A. J. E. Reversible calcium-regulated stopcocks in legume sieve tubes. *Plant Cell* **13**, 1221–1230 (2001).
23. Knoblauch, M., Stubenrauch, M., van Bel, A. J. E. & Peters, W. S. Forisome performance in artificial sieve tubes. *Plant Cell Environ.* **35**, 1419–1427 (2012).
24. Rüping, B. et al. Molecular and phylogenetic characterization of the sieve element occlusion gene family in *Fabacea* and non-*Fabaceae* plants. *BMC Plant Biol.* **10**, 219 (2010).
25. Froelich, D. R. et al. Phloem ultrastructure and pressure flow: Sieve-element-occlusion-related agglomerations do not affect translocation. *Plant Cell* **23**, 4428–4445 (2011).
26. Ernst, A. M. et al. Sieve element occlusion (SEO) genes encode structural phloem proteins involved in wound sealing of the phloem. *Proc. Natl. Acad. Sci. U. S. A.* **109**, E1980–E1989 (2012).
27. Jekat, S. B. et al. P-proteins in *Arabidopsis* are heteromeric structures involved in rapid sieve tube sealing. *Front. Plant Sci.* **4**, 225 (2013).
28. Musetti, R. et al. Phytoplasma-triggered $Ca^{2+}$ influx is involved in sieve- tube blockage. *Mol. Plant-Microbe Interact.* **26**, 379–386 (2013).
29. de Wit, P. How plants recognize pathogens and defend themselves. *Cell. Mol. Life Sci.* **64**, 2726–2732 (2007).
30. Schulz, P., Herde, M. & Romeis, T. Calcium-dependent protein kinases: Hubs in plant stress signaling and development. *Plant Physiol.* **163**, 523–530 (2013).
31. McCormack, E., Tsai, Y. C. & Braam, J. Handling calcium signaling: *Arabidopsis* CaMs and CMLs. *Trends Plant Sci.* **10**, 383–389 (2005).
32. Tortosa, M., Cartea, M. E., Velasco, P., Soengas, P. & Rodriguez, V. M. Calcium-signaling proteins mediate the plant transcriptomic response during a well-established *Xanthomonas campestris* pv. *campestris* infection. *Hortic. Res.* **6**, 103 (2019).
33. Benjamins, R., Ampudia, C. S., Hooykaas, P. J. & Offringa, R. PINOID-mediated signaling involves calcium-binding proteins. *Plant Physiol.* **132**, 1623–1630 (2003).
34. Ma, W., Smigel, A., Tsai, Y. C., Braam, J. & Berkowitz, G. A. Innate immunity signaling: Cytosolic $Ca^{2+}$ elevation is linked to downstream nitric oxide generation through the action of calmodulin or a calmodulin-like protein. *Plant Physiol.* **148**, 818–828 (2008).
35. Sun, L., Qin, J., Wu, X., Zhang, J. & Zhang, J. TOUCH 3 and CALMODULIN 1/4/6 cooperate with calcium-dependent protein kinases to trigger calcium-dependent activation of CAM-BINDING PROTEIN 60-LIKE G and regulate fungal resistance in plants. *Plant Cell* **34**, 4088–4104 (2022).
36. Pandey, S. Characterization and expression analysis of the calmodulin protein, CAM2, in *Arabidopsis thaliana*. *Int. J. Innov. Sci. Res. Technol.* **8**, 1298–1313 (2023).

37. Meena, M. K. et al. The $Ca^{2+}$ channel CNGC19 regulates *Arabidopsis* defense against *Spodoptera* herbivory. *Plant Cell* **31**, 1539–1562 (2019).
38. Yip Delormel, T. & Boudsocq, M. Properties and functions of calcium-dependent protein kinases and their relatives in *Arabidopsis thaliana*. *New Phytol.* **224**, 585–604 (2019).
39. Lee, H., Ganguly, A., Baik, S. & Cho, H. T. Calcium-dependent protein kinase 29 modulates PIN-FORMED polarity and *Arabidopsis* development via its own phosphorylation code. *Plant Cell* **4**, 3513–3531 (2021).
40. Genot, B. et al. Constitutively active *Arabidopsis* MAP Kinase 3 triggers defense responses involving salicylic acid and SUMM2 resistance protein. *Plant Physiol.* **174**, 1238–1249 (2017).
41. Asai, T. et al. MAP kinase signalling cascade in *Arabidopsis* innate immunity. *Nature* **415**, 977–983 (2002).
42. Xu, J. & Zhang, S. Regulation of ethylene biosynthesis and signaling by protein kinases and phosphatases. *Mol. Plant* **7**, 939–942 (2014).
43. Wang, J. et al. CARK6 is involved in abscisic acid to regulate stress responses in *Arabidopsis thaliana*. *Biochem. Biophys. Res. Commun.* **513**, 460–464 (2019).
44. van Mourik, H. et al. Divergent regulation of *Arabidopsis SAUR* genes: A focus on the *SAUR10*-clade. *BMC Plant Biol.* **17**, 245 (2017).
45. Stortenbeker, N. & Bemer, M. The SAUR gene family: The plant's toolbox for adaptation of growth and development. *J. Exp. Bot.* **70**, 17–27 (2019).
46. Argueso, C. T. & Kieber, J. J. Cytokinin: From autoclaved DNA to two-component signaling. *Plant Cell* **36**, 1429–1450 (2024).
47. Großkinsky, D. K. & Petrášek, J. Auxins and cytokinins—the dynamic duo of growth-regulating phytohormones heading for new shores. *New Phytol.* **221**, 1187–1190 (2019).
48. Yang, T. & Poovaiah, B. W. Molecular and biochemical evidence for the involvement of calcium/calmodulin in auxin action. *J. Biol. Chem.* **275**, 3137–3143 (2000).
49. Vanneste, S. & Friml, J. Calcium: The missing link in auxin action. *Plants* **2**, 650–675 (2013).
50. Huot, B., Yao, J., Montgomery, B. L. & He, S. Y. Growth-defense tradeoffs in plants: A balancing act to optimize fitness. *Mol. Plant* **7**, 1267–1287 (2014).
51. Attaran, E. & He, S. Y. The long-sought-after salicylic acid receptors. *Mol. Plant* **5**, 971–973 (2012).
52. Rivas-San Vicente, M. & Plasencia, J. Salicylic acid beyond defense: Its role in plant growth and development. *J. Exp. Bot.* **62**, 3321–3338 (2011).
53. Pattyn, J., Vaughan-Hirsch, J. & van de Poel, B. The regulation of ethylene biosynthesis: A complex multilevel control circuitry. *New Phytol.* **229**, 770–782 (2021).
54. Gao, M., Hao, Z., Ning, Y. & He, Z. Revisiting growth-defense trade-offs and breeding strategies in crops. *Plant Biotechnol. J.* **22**, 1198–1205 (2024).
55. Perdiguero, P. et al. Gene expression trade-offs between defense and growth in English elm induced by *Ophiostoma novo-ulmi*. *Plant Cell Environ.* **41**, 198–214 (2018).
56. Wang, S. et al. Crystal structure of calsequestrin from rabbit skeletal muscle sarcoplasmic reticulum. *Nat. Struct. Biol.* **5**, 476–483 (1998).
57. Heizmann, C. W. & Hunzlker, W. Intracellular calcium-binding proteins: More sites than insights. *Trends Biochem. Sci.* **16**, 98–103. https://doi.org/10.1016/0968-0004(91)90041-S (1991).
58. Valeyev, N. V., Bates, D. G., Heslop-Harrison, P., Postlethwaite, I. & Kotov, N. V. Elucidating the mechanisms of cooperative calcium-calmodulin interactions: A structural systems biology approach. *BMC Syst Biol.* **2**, 48 (2008).
59. Wright, P. E. & Dyson, H. J. Intrinsically disordered proteins in cellular signaling and regulation. *Nat. Rev. Mol. Cell Biol.* **16**, 18–29 (2015).
60. Guo, M., Kim, P., Li, G., Elowsky, C. G. & Alfano, J. R. A bacterial effector co-opts calmodulin to target the plant microtubule network. *Cell Host Microbe* **19**, 67–78 (2016).
61. Carella, P., Wilson, D. C. & Cameron, R. K. Some things get better with age: Differences in salicylic acid accumulation and defense signaling in young and mature *Arabidopsis*. *Front. Plant Sci.* **5**, 775 (2015).
62. Wilson, D. C., Kempthorne, C. J., Carella, P., Liscombe, D. K. & Cameron, R. K. Age-related resistance in *Arabidopsis thaliana* involves the MADS-domain transcription factor SHORT VEGETATIVE PHASE and direct action of salicylic acid on *Pseudomonas syringae*. *Mol. Plant-Microbe Interact.* **30**, 919–929 (2017).
63. Salinas, P., Velozo, S. & Herrera-Vásquez, A. Salicylic acid accumulation: Emerging molecular players and novel perspectives on plant development and nutrition. *J. Exp. Bot.* https://doi.org/10.1093/jxb/erae309 (2024).
64. Mullendore, D. L. et al. Non-dispersive phloem-protein bodies (NPBs) of *Populus trichocarpa* consist of a SEOR protein and do not respond to cell wounding and $Ca^{2+}$. *PeerJ* **6**, e4665 (2018).
65. Knoblauch, M., Peters, W. S., Bell, K., Ross-Elliott, T. J. & Oparka, K. J. Sieve-element differentiation and phloem sap contamination. *Curr. Opin. Plant Biol.* **43**, 43–49 (2018).
66. Liao, Y., Smyth, G. K. & Shi, W. featureCounts: An efficient general porpuose program for assigning sequence reads to genomic features. *Bioinformatics* **30**, 923–930 (2014).
67. Vandesompele, J. et al. Accurate normalization of real-time quantitative RT-PCR data by geometric averaging of multiple internal control genes. *Genome Biol.* https://doi.org/10.1186/gb-2002-3-7-research0034 (2002).
68. Pfaffl, M. W. A new mathematical model for relative quantification in real-time RT-PCR. *Nucleic Acids Res.* **29**, e45 (2001).
69. Lee, I. M. et al. '*Candidatus* Phytoplasma asteris', a novel phytoplasma taxon associated with aster yellows and related diseases. *Int. J. Syst. Evol. Microbiol.* **54**, 1037–1048 (2004).
70. Martini, M. et al. Ribosomal protein gene-based phylogeny for finer differentiation and classification of phytoplasmas. *Int. J. Syst. Evol. Microbiol.* **57**, 2037–2051 (2007).
71. Pacifico, D. et al. Decreasing global transcript levels over time suggest that phytoplasma cells enter stationary phase during plant and insect colonization. *Appl. Environ. Microbiol.* **81**, 2591–2602 (2015).
72. MacLean, A. M. et al. Phytoplasma effector SAP54 induces indeterminate leaf-like flower development in *Arabidopsis* plants. *Plant Physiol.* **157**, 831–841 (2011).
73. Jollard, C. et al. Flavescence dorée phytoplasma has multiple *ftsH* genes that are differentially expressed in plants and insects. *Int. J. Mol. Sci.* **21**, 150 (2020).
74. Launay, G. & Simonson, T. Homology modelling of protein-protein complexes: A simple method and its possibilities and limitations. *BMC Bioinform.* **9**, 427 (2008).
75. Bordoli, L. et al. Protein structure homology modeling using SWISS-MODEL workspace. *Nat. Protoc.* **4**, 1–13 (2009).
76. Koch, I., Philipp, O., Hamann, A. & Osiewacz, H. Reconstruction of protein–protein interaction networks using homology-based search: application to the autophagy pathway of aging in *Podospora anserina*. In: Canzar S. & Rojas Ringeling F. (eds.), Protein-protein interaction networks: Methods and Protocols, Methods in Molecular Biology, vol. 2074, pp. 45–55 (2020). © Springer Science+Business Media, LLC, part of Springer Nature 2020.


## Acknowledgements

This work was supported by the University of Padova, Ricerca Scientifica DOR, prot. DOR2228571 and DOR2381035. Figure 8 is created in BioRender.com

## Author contributions

R.M. conceived and supervised the project. K.O. carried out RNA-seq data analysis and constructed the interaction networks. F.R.C. grew the plants and collected the samples. O.C.V. designed and performed RT-qPCR experiments. R.M. and A.J.E.vB. wrote the manuscript, with the valuable contribution of S.S. All the authors provided critical suggestions for the realization of the manuscript.

## Declarations

## Competing interests

The authors declare no competing interests.

## Additional information

**Supplementary Information** The online version contains supplementary material available at https://doi.org/10.1038/s41598-025-01374-8.

**Correspondence** and requests for materials should be addressed to R.M.

**Reprints and permissions information** is available at www.nature.com/reprints.

**Publisher's note** Springer Nature remains neutral with regard to jurisdictional claims in published maps and institutional affiliations.